COMPLEX DIELECTRIC PERMITTIVITY OF SOILS AS A FUNCTION OF WATER CONTENT AT MICROWAVE FREQUENCIES

*Dissertation submitted to the Jawaharlal Nehru University
in partial fulfilment of the requirement for
the award of the Degree of*

MASTER OF PHILOSOPHY

ANIRBID GHOSH

SCHOOL OF ENVIRONMENTAL SCIENCES
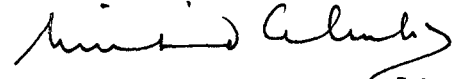### JAWAHARLAL NEHRU UNIVERSITY
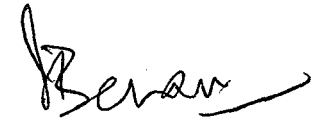### NEW DELHI - 110067
INDIA

1996

CERTIFICATE

Certified that the work embodied in this dissertation entitled "**Complex Dielectric Permittivity of soils as a Function of Water at Microwave Frequencies**" has been carried by me under the supervision of Prof. J. Behari in the School of Environmental Sciences, Jawaharlal Nehru University, New Delhi. The work is original and has not been submitted in part or full for any other degree or diploma in this or any other university.

Anirbid Ghosh

Prof. P. S. Ramakrishnan
(Dean, S.E.S)

Prof. J. Behari
(Supervisor)

To

Baba
and
Ma

CONTENTS

I

ACKNOWLEDGEMENT

CHAPTER I

INTRODUCTION

Over the past three decades, *microwave remote sensing* has evolved into an important tool for monitoring the atmosphere and surface of planetary objects, with special emphasis on observation of the planet earth. The term "microwave remote sensing" encompasses the physics of radiowave propagation in and their interaction with material media. This may also include surface and volume scattering and emission techniques used for designing microwave sensors and processing the data they acquire, and the translation of the measured data into information about the temporal or spatial variation of atmospheric, surface and medium parameters or properties.

Microwave sensors can be of two types:

(1) *Active* sensors are those that provide their own source of illumination and therefore contain a transmitter and a receiver.

(2) *Passive* sensors are simply receivers that measure the radiation emanating from the scene under observation. Active microwave sensors include *radar imagers, scatterometers* and *altimeters*. Passive microwave sensors and often referred to as *microwave radiometers*.

Significance of soil moisture content studies:

Soil moisture plays a vital role in the functioning of ecosystems and in mass and energy exchange processes occurring at the land-atmosphere interface. Thus, knowledge of the temporal and spatial variations of soil moisture is an important input to predictive models and management policies in disciplines like hydrology, agriculture and climatology.

Soil moisture is a critical parameter that determines the partitioning of heat and moisture atmospheric forcing at the land surface boundary. Moreover, soil moisture content is an important parameter is many industrial and mining processes as well as for understanding the global hydrologic cycle and its effect on weather and climate.

Microwaves and their relevance in the study of soil moisture content:

Microwaves refer to electromagnetic radiation of frequencies ranging from several hundred MHz to several hundred GHz. Microwaves have been put to various uses depending mainly upon the selected frequency range. Some of the practical applications are:

(a) Microwave oven at around 2.4 GHZ.

(b) Microwave relay telephone at arround 4.0 GHZ.

(c) Satellite television at around 4 GHZ (down link).

(d) Satellite television at around 6 GHZ (uplink).

(e) Police radar at around 22 GHZ.

An important characteristic of microwave signals that makes them so universally applicable is that they can propagate through the ionosphere with minimum loss (water vapor, ozone, and oxygen absorb microwaves of certain frequencies).

On the other hand at frequencies below the microwave range, e.m. radiation is reflected back by the ionosphere. This property makes microwaves most suited for spacebound communications as well as satellite remote sensing.

Failure of soil moisture studies in non-microwave regions is due to the following reasons:

(a) The reflection co-efficient is less sensitive to soil moisture variations in the visible region compared to its equivalent parameters like reflectivity and emissivity in other regions of the e.m. spectrum.

(b) Atmospheric scattering and attenuation (which is extremely difficult to accurately account for) are higher.

3

(c) Reflection coefficient is highly sensitive to soil surface roughness, feature and vegetation cover variation.

Most of these difficulties are either overcome or simplified in the microwave region. The atmosphere is almost completely transparent to microwaves. Besides, they can penetrate deep into the soils and multi-frequency and multi-polarization approaches are possible. Through various field and aircraft experiments, it has been demonstrated that the proper choice of frequency, look-angle and polarization minimizes the effect of surface roughness.

Microwave sensors offer the potential for remote sensing of soil moisture because of the large change the addition of water makes to the dielectric constant of dry soil (cf: Dobson et al., 1985; Jackson et al., 1989; and others).

The dielectric constant of water is approx. 80 compared with 3 to 5 for dry soil. This large dielectric constant of liquid water is due to the alignment of the electric dipole moments of water molecules in response to an applied field. Dielectric constant of soil therefore increases with its moisture content. The sensitivity of microwave response to soil moisture variation coupled with the relative transparency of the atmosphere (< 90%) towards microwaves

make microwave sensors well suited for remote sensing of soil.

THE PRESENT WORK.

The diversity of a country so vast as India is reflected in its landscape, and climatic conditions. Such divergent physiographic conditions are also reflective in the evolution of different types of soil and vegetation in its different parts.

Nature of soil and its properties like soil depth, texture, organic matter content and mineralogical composition control its water holding capacity which is of utmost importance for plant life. As has already been discussed, soil moisture information is important for the agricultural scientist, the remote sensing scientist, the geologist and the meteorologist. Much work has already been done abroad on soil moisture studies through dielectric constant measurements. In India, however, this kind of work needs to make a lot of headway.

Dielectric Constant of soil is dependent upon the microwave frequency, temperature, salinity, relative fraction of bound and free water, bulk density, shape and size of soil particles, etc.

In the present work, dielectric parameters of soil samples collected from different regions of India have been

measured at different moisture contents at KU band frequencies (around 15 GHz). The measurements have been carried out by two different methods, viz. The wave guide method involving two point solution of a transcendental equation, and the single horn reflectometry method. Effects of soil texture on such measurements if any has also been looked into. Parameters like *field capacity* and *wilting point* useful to agricultural scientists have also been calculated.

The purpose of this work is to prepare a data bank on Indian soils and to prepare the groundwork for future field investigations. The present work, it is believed, will be of utility to both remote sensing scientists and agricultural scientists.

CHAPTER II

THEORETICAL BACKGROUND

Importance of Dielectric Constant Measurements:

Dielectric studies of material has been a powerful tool in assessing the structure and behaviour of molecular materials (Von Hippel, 1961). The response of a material to an applied electromagnetic field is determined by the electrical and magnetic properties of the medium. For a non-magnetic system, the significant property which determines the impedance offered to the incident wave is the dielectric constant of the medium. If the medium is lossy, energy is absorbed as the radiation penetrates the material. The amplitude of the wave decreases, i.e., attenuation occurs as energy is absorbed. This is accompanied by a shift in phase. The attenuation and phase shift are dependent on the dielectric properties of the medium characterized by the complex permittivity of the medium denoted as, $\epsilon'-j\epsilon''$. (Here, ϵ' is the real permittivity, the dielectric constant of an equivalent lossless dielectric and ϵ'' is the loss factor). The complex permittivity is frequency dependent.

The Debye Theory:

The present understanding of the dielectric properties

of materials is based mostly on the Debye theory (Smyth, 1955; Bottcher, 1952), of relaxing dipole interacting with an applied electric field. Early work showed that a set of exactly equivalent, non-interacting dipoles characterized by a single relaxation time τ adequately explained the behaviour of weak dipolar solutions or dipolar molecules in the gaseous phase, but was insufficient to account for the broader frequency range over which dispersion was observed in solids and liquids in the frequency range below -10^{10} Hz. This difficulty was circumvented by a consideration of distribution of relaxation times, like Cole-Cole, Fuoss-Kirkwood, Cole-Davidson and William-Watts treatments (Hill, et.al., 1969; Bottcher, et.al., 1978), applied to the case of more interactive media. Such approaches involve interpretation of the experimental measurements in terms of degree of fit to empirical functions. An empirical characterization of loss in solids and liquids was proposed by Jonscher (1977) and a more generalised expression was proposed by R.M.Hill (1978). The various types of dielectric response has been summarised by Ngai et al.,(1979). At one extreme is the case of non-interacting system characterized by Debye behaviour. Increasing nearest neighbour interaction lead to behaviour as postulated by Cole and Cole or Cole and -Davidson. (Hill et al., 1969;

Bottcher et al., 1978). Finally, as the interactions tend to be more complicated as in the case of solids and solid like substances, universal dielectric response suggested by Jonscher (1977) seems to be applicable.

The Debye Equation

When a system of dipolar molecules is placed in a static field, the polarization will be in equilibrium with the field. If the field is alternating at low frequencies, the polarization will still be in phase with the electric field. If the frequency is sufficiently large the polarization will lag behind the applied field leading to absorption of energy and fall in permittivity. It was assumed that if there is a polarization in the absence of an electric field, due to the occurrence of a field in the past, the decrease of the orientation polarization depends only on the value of the orientation polarization at that instant. Assuming the rate of change of polarization to be proportional to the polarization, the differential equation for the orientation polarization in the absence of an electric field is

$$\frac{d\ P_{or}(t)}{dt} = -\frac{1}{\tau}\ P_{or}(t) \qquad \dots (2.1)$$

Where τ^{-1} is the constant of proportionality which has dimensions of a reciprocal time. The solution of eq. (2.1) leads to an exponential form

$$P_{or}(t) = P_{or}(0) \; e^{-\, t/\tau} \qquad \qquad \ldots (2.2)$$

In the reverse situation when the polarization is built up due to application of a constant external field

$$P_{or}(t) = P_{or}(\infty) \; \{1 - e^{-t/\tau}\} \qquad \qquad \ldots (2.3)$$

The total polarization P_S in a static field E may be divided into two parts.

$$P_S = P_\infty + P_{or}. \qquad \qquad \ldots (2.4)$$

Where P_{or} indicates the part of P_S due to dipole orientation and P_∞ the part due to the polarizability of the particles. Neglecting the time required to establish P_∞ relative to the time required to build up P_{or}, we may consider P_{or}, to be built up in the time in which P_∞ changes to P_S. The electric displacement D is related to the applied electric field E and polarization P by,

$$D = E + 4\pi P \qquad \qquad \ldots (2.5)$$

Since, in the static case $D_S = \epsilon_S E$ where ϵ_S is the static permittivity of the medium,

$$P_S = \frac{\epsilon_S - 1}{4\pi} E \qquad \qquad \ldots (2.6)$$

Similarly, the refractive index n_∞ is defined in terms of P_∞ as

$$P_\infty = \frac{n^2 - 1}{4\pi} E \qquad \ldots (2.7)$$

with $n_\infty^2 = \epsilon_\infty$

The theory of dielectric relaxation is based on the assumption that eq (2.3) is also valid for an alternating field. Representing the alternating field by $E(t)$, eq. (2.4) with the help of eq. (2.6) and (2.7) becomes

$$P_{or} = \frac{\epsilon_s - 1}{4\pi} E(t) - \frac{\epsilon_\infty - 1}{4\pi} E(t) \qquad \ldots (2.8)$$

If the field is alternating with a frequency it can be represented by

$$E(t) = E_o e^{jwt} \qquad \ldots (2.9)$$

The differential equation for the build up of polarization would then become

$$\frac{d\bar{P}_{or}(t)}{dt} = \frac{1}{\tau} \left\{ \frac{\epsilon_s - \epsilon_\infty}{4} E_o e^{jwt} - \bar{P}_{or}(t) \right\} \qquad \ldots (2.10)$$

The general solution of this equation is

$$P_{or}(t) = Ce^{-t/\tau} + \frac{1}{4\pi} \frac{\epsilon_s - \epsilon_\infty}{1 + jw\tau} E_o e^{jwt} \qquad \ldots (2.11)$$

The first term on the right hand side will decrease to an infinitely small value after some time and therefore, can be neglected. Thus the total polarization is,

$$\bar{P} = \bar{P}_\infty + \bar{P}_{or}(t)$$

$$= \left\{ \frac{\epsilon_\infty - 1}{4\pi} + \frac{1}{4\pi} \cdot \frac{\epsilon_s - \epsilon_\infty}{1 + jw\tau} \right\} E_o e^{jwt} \qquad \ldots (2.12)$$

11

Thus, **P** is a sinusoidal function of time with the same frequency as that of the applied field but lagging in phase with respect to **E**. Eq. (2.5) can be generalized for alternating fields. It then leads to

$$\overline{D} = \overline{E} + 4\pi\overline{P}$$

$$= \left\{\epsilon_\infty + \frac{\epsilon_s - \epsilon_\infty}{1 + jw\tau}\right\} E_0\, e^{jwt} \qquad \ldots (2.13)$$

Expressing the complex displacement **D** as $D = \epsilon^* \times E$, the complex permittivity $\epsilon^*(w)$ is given by

$$\epsilon^*(w) = \epsilon' - j\epsilon'' = \epsilon_\infty + \frac{\epsilon_s - \epsilon_\infty}{1 + jw\tau} \qquad \ldots (2.14)$$

Which leads to

$$\epsilon' = \epsilon_\infty + \frac{\epsilon_s - \epsilon_\infty}{1 + w^2\tau^2} \qquad \ldots (2.15a)$$

and

$$\epsilon'' = \frac{(\epsilon_s - \epsilon_\infty)w\tau}{1 + w^2\tau^2} \qquad \ldots (2.15b)$$

According to equations (2.15), ϵ' will decrease from ϵ_s to ϵ_∞ whereas ϵ'' will become maximum at $w\tau = 1$. A plot of ϵ' and ϵ'' against log w would be symmetrical. A method for checking eq. (2.15) was proposed by Cole and Cole. From egs. (2.15), it is evident that a plot of ϵ'' vs ϵ' should be a semi-circle with radius $(\epsilon_s - \epsilon_\infty)/2$, and centre beeing on the abscissa at a distance of $(\epsilon_s - \epsilon_\infty)/2$ from the origin.

Departure from Debye Behaviour

Although eqs. (2.15) gives an adequate description of the behaviour of orientation polarization for a large number of condensed systems, for many other systems marked deviations occur. This is evident from the occurrence of more than one maximum in ϵ'' as a function of frequency. The deviations occur due to a distribution of relaxation times either distinct from each other or closely spaced such that they are not directly evident. Cole-Cole suggested the following empirical modifications to eq. (2.14).

$$\epsilon^*(w) = \epsilon_\infty + \frac{\epsilon_s - \epsilon_\infty}{(1+jw\tau)^{1-h}} \qquad \ldots (2.16)$$

This leads to a depressed semicircular arc plot of ϵ'' against ϵ'. The factor h being related to the depression of the centre from the ϵ' axis. Another generalized expression was given by Davidson and Cole

$$\epsilon^*(w) = \epsilon_\infty + \frac{\epsilon_s - \epsilon_\infty}{(1+jw\tau)^\beta} \qquad \ldots \ldots (2.17)$$

The Cole-Cole plot for the above equation is asymmetric and is often called a skewed arc. At low frequencies the plot cuts the ϵ' axis perpendicularly, whereas, on the high frequency side at an angle $\pi\beta/2$. The maximum of $\epsilon''(w)$ is found for a value of $w > \tau^{-1}$. Some of the descriptions of relaxation behaviour have been proposed for experimentally

measurable function other than $\epsilon^*(w)$. Expressions for loss factor $\epsilon''(w)$ were suggested by Fuoss and Kirkwood, and Jonscher, and for the step response function was proposed by Williams and Watts. Bottcher and Bordewijk (1978) and Hill et al. (1969) have given a detailed description of the various function proposed for explaining the departure from Debye behaviour.

Properties of Soil and its Relationship with Water:

Soil is the weathered and fragmented outer layer of the earth's surface, formed from disintegration and decomposition of rocks by physical and chemical processes, and influenced by the activity and accumulated residues of innumerous biological species. A typical characteristic of soil which plays an important role in determining the nature of its interaction with water is its very large interfacial area per unit volume. This is due to the fact that soil is a heterogeneous, polyphasic, particulated, disperse and porous system.

Three Phases of the Soil System

Like ordinary water the soil system also exhibits three phases, viz, the solid phase, consisting of soil particles; the liquid phase, consisting of soil water and along with it dissolved substances; and lastly the gaseous phase consisting of soil air.

14

Soil is thus an exceedingly complex system. The solid matrix of the soil system consists of particles differing in chemical and mineralogical composition as well as in size, shape and orientation. The mutual arrangement of these particles determines the characteristics of the pore spaces in which water and air are transmitted or retained.

Soil Texture

The texture of a soil is determined by the size or size range of the particles. In other words, soil texture is the relative proportion of various sizes of particles present in it. Traditionally, soil is divided into 3 particle size ranges: Sand, silt and clay. Although a number of soil classification schemes are in use, for the present work, we shall follow the U.S. Department of Agriculture classifications (Fig 2:1):

Sand : $d > 0.05$ mm

Silt : $0.002 < d < 0.05$ mm

Clay : $d < 0.002$ mm

Here "d" refers to the particle diameter. Soils having different compositions of the three basic particles sand, silt and clay are assigned different groupings as shown in (Fig.2.2)

Porosity

Soil porosity (P) is defined as $P = V_f / V_t$ where "V_f" is

International Soil Science Society Classification
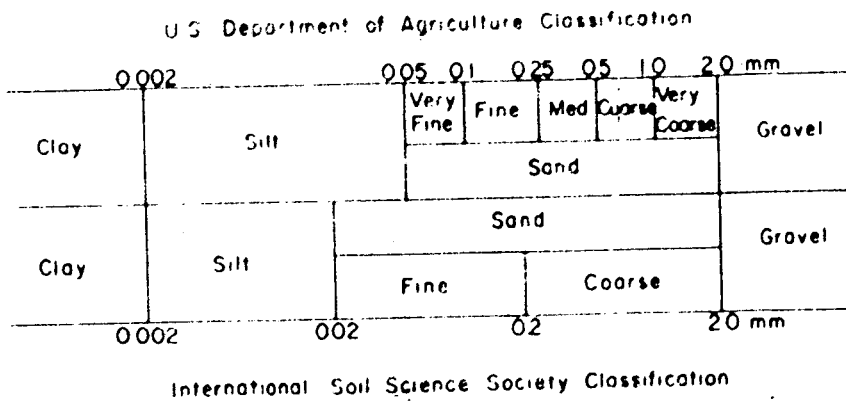
Fig. 2.1: Textural classification of soil fractions according to particle diameter ranges.
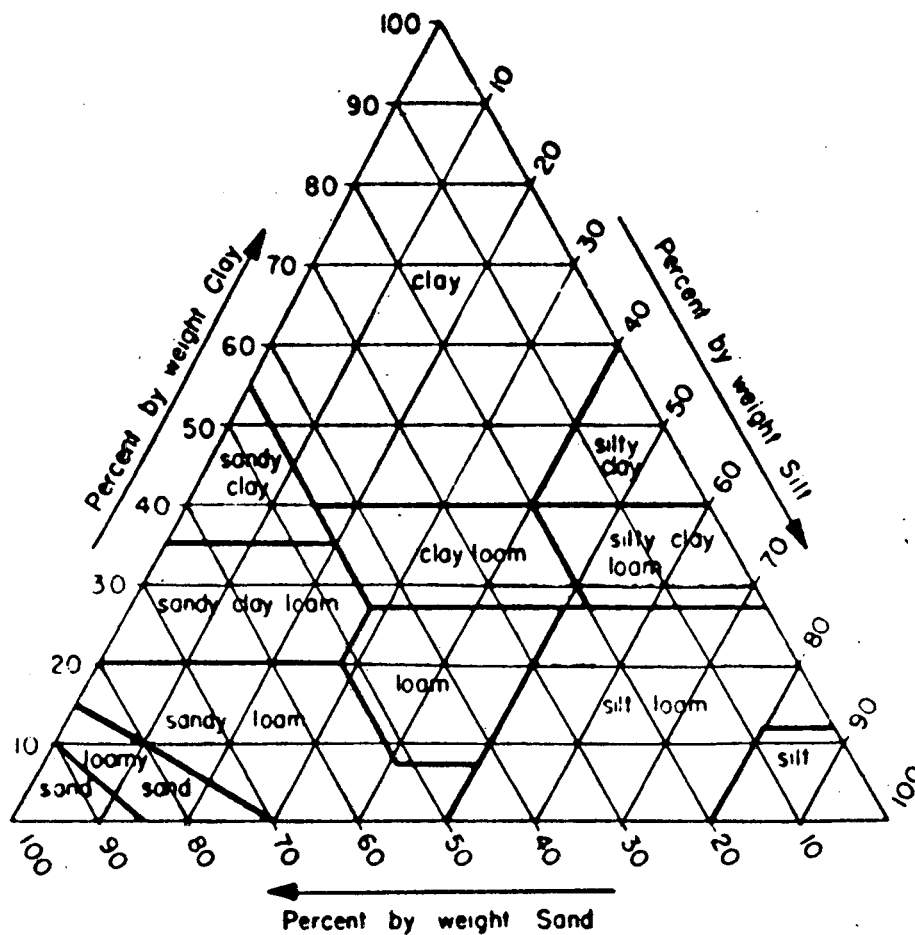
Fig. 2.2: Textural triangle showing the percentage of clay, silt and sand in the basic soil textural classes.

the volume of pores and `$V_t$` is the total volume of soil. The value of P varies between 0.3 - 0.6 (30-60%).

Coarse textured soils have less porosity than fine textured soils in spite of the fact that the mean dimension of individual pores is greater for coarse textured soils. The term porosity, thus refers to the volume fraction of pores.

The Clay fraction and its characteristic properties

The clay fraction of soil has the largest specific surface area amongst the other fraction (viz., silt and sand) and hence, it actively participates in all physico-chemical processes undergone by the soil system. Due to its inherent property clay absorbs water and causes the soil to swell and shrink upon wetting and drying (Grim, 1958). Clay particles are mostly negatively charged and form an electrostatic double layer with the exchangeable cations.

The sand and silt particles on the other hand are larger in size and are mineralogically composed mainly of quartz and other primary mineral particles which have not been transformed chemically into secondary minerals as in the case of clay. Clay, thus differs texturally as well as mineralogically from sand and silt.

Clay mostly consists of layered alumino silicate crystals which are composed of two basic structural units (Grim, 1963; Marshall, 1964: Low, 1968). :

(i) a tetrahedron of oxygen atoms surrounding a central cation, usually Si^{+4}, and

(ii) an octahedron of oxygen atoms of hydroxyl groups surrounding a larger cation, usually Al^{+3} or Mg^{+2}.

The tetrahedra are joined at their basal corners and the octahedra are joined along their edges by means of shared oxygen atoms. (Fig. 2.3)

The layered aluminosilicate minerals are of two types depending on the ratios of tetrahedral to octahedral layers, whether 1:1 or 2:1. In the 1:1 minerals like Kaolinite, an octahedral layer is attached by the sharing of oxygen to a single tetrahedral layer. In the 2:1 minerals like montmorillonite, it is attached in the same way to two tetrahedral layers, one on each side. The multiple-stacked composite layer (or unit cells) of this sort, are called lamellae.

In reality some isomorphous replacements of Al^{+3} for Si^{+4} in the tetrahedral layers and of Mg^{+2} for Al^{+3} in the octahedral layers take place in this idealized structure leading to internally unbalanced negative charges at different sites in the lamellae. The incomplete charge

60
4 Si

40·2 OH

4 Al

6 OH

Kaolinite

60
4 Si

40·2 OH

4 Al

40·2 OH

4 Si

60

Montmorillonite
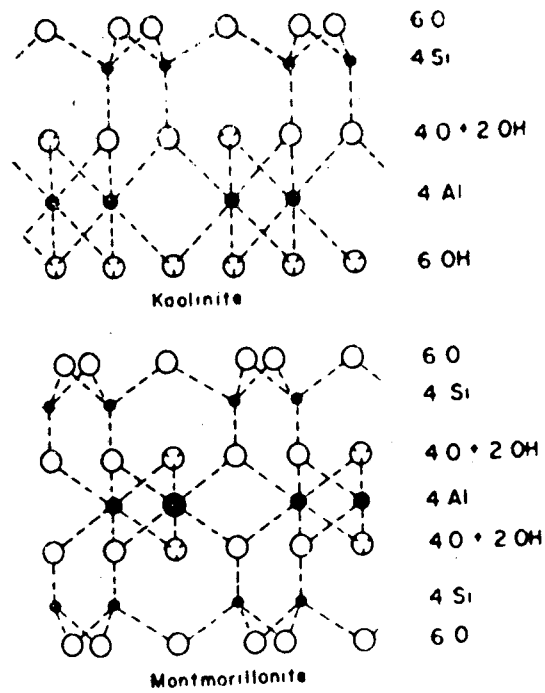
Fig. 2.3: Schematic representation of the structure of aluminosilicate minerals.

Positive ions (+)

n_0

Negative ions (-)

Distance from micelle surface
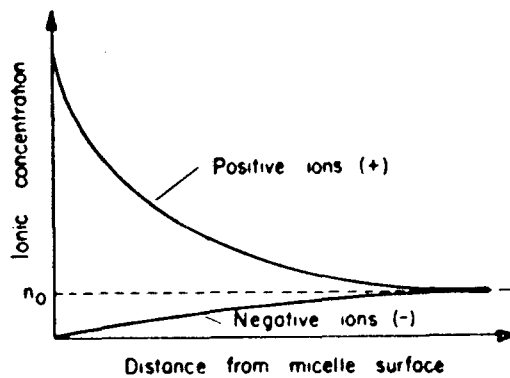
Fig. 2.4: Distribution of positive and negative ions in solution with distance from the surface of a clay micelle bearing net negative charge. (n_0 is the ionic concentration in the bulk solution outside the electrical double layer)

neutralization of terminal atom on lattice edges also produces unbalanced charge. These charges are balanced externally by exchangeable ions (mostly cations), concentrating near the external surfaces of the particle and occasionally penetrating into interlamellar spaces. These cations do not form an integral part of the lattice structure, and can be replaced, or exchanged, by other cations. This cation exchange process is of utmost importance in the physico-chemistry of soil, as it affects the retention and release of nutrients and salts, and the flocculation-dispersion processes of soil colloids.

A hydrated clay particle forms a colloidal micelle, in which the excess negative charge of the particle surface and the neutralizing cation form an electrostatic double layer. The cation swarm consists partly of a layer more or less fixed in the proximity of the particle surface (known as the Stern layer), and partly of a diffuse distribution extending some distance away from the particle surface (fig. 2.4). This kind of distribution results from an equilibrium between two opposing effects; the Coulomb attraction of the clay particle against the Brownian motion of the liquid molecules, inducing outward diffusion of the cations toward the intermicellar solution. Just as cations are adsorbed positively toward the clay particles, so anions are

repelled, or adsorbed negatively, and relegated from the micellar to the inter micellar solution. The quantity of cations adsorbed on soil-particle surfaces per unit mass of the soil under chemically neutral conditions is nearly constant and independent of the species of cation, and is generally known as the cation exchange capacity. Soils vary in cation exchange capacity from nil to perhaps 0.60 mEq per gm (Bear, 1955).

Clay minerals differ some what in surface charge density (i.e., the number of exchange sites per unit area of particle surface), and differ greatly in specific surface area. Hence, they differ also in their total cation-exchange capacity. Montmorillonite with a specific surface area of nearly $800m^2/gm$, has a cation-exchange capacity of about 0.95 mEq/gm, whereas kaolinite has an exchange capacity of only 0.04-0.09 mEq/gm. The greater specific surface area of montmorillonite is due to its lattice expansion and consequent exposure of internal (interlamellar) surfaces, which are not so exposed in the case of kaolinite. Other clay minerals (eg: illite, micas, palygorskite) often exhibit properties intermediate between those of kaolinite and montmorillonite.

The attraction of a cation to a negatively charged clay micelle generally increases with increasing valency of the

cation. Thus, monovalent cation are replaced more early than divalent or trivalent cations. Highly hydrated cations, which tend to be farther from the surface, are also more easily replaced than less hydrated ones. The order of preference of cations in exchange reactions is generally as follows:

$$Al^{3+} > Ca^{2+} > Mg^{2+} > K^+ > Na^+ > Li^+$$
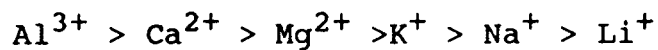
When confined clay are allowed to absorb water, swelling pressures develop, which are related to the osmotic pressure difference between the double layer and the external solution. Depending upon their state of hydration and the composition of their exchangeable cations, clay particles may either flocculate or disperse. Dispersion generally occurs with monovalent and highly hydrated cations (eg., sodium). Conversely, flocculation occurs at high solute concentrations and/or in the presence of divalent and trivalent cation (eg., Ca^{2+}, Al^{3+}) when the double layer is compressed and any two micelles can approach each other more closely. Thus, the short-range attractive forces (known as van der Waal's forces) can come into play and join the indi vidual micelles into flocs.

Water Adsorption on Solid Surface

Adsorption is a type of interfacial phenomenon resulting from the differential forces of attraction or

repulsion occurring among molecules of different phases at their contact surfaces. As a result of these cohesive and adhesive forces, the contact zone may exhibit a concentration or a density of material different from that inside the phases them selves.

The interfacial forces of attraction or repulsion coming into play during adsorption phenomenon may be of different kinds, viz., electrostatic or ionic (Coulomb) forces, intermolecular van der Waal's or London forces, and short range repulsive (Born) forces.

Water adsorption upon solid surfaces is electrostatic in nature. The polar water molecules attach themselves to the charged faces of the solids. It is due to adsorption of water that clay soils exhibit a strong retention capacity of water. The interaction of the charges of the solid with the polar water molecules may impart a distinct and rigid structure in which the water dipoles assume an orientation dictated by the charge sites on the solids. This adsorbed layer of water may have mechanical properties of strength and viscosity different from those of ordinary liquid water at same temperatures.

Some Parameters Connected with Soil Moisture Retention under Field Conditions

(i) **Field Capacity** : After a soil has been wetted due to rain or irrigation there is a constant rapid downward

TH-6384

movement of a portion of the water (internal drainage) due to existence of a hydraulic gradient. After a few days this movement stops. The presumed water content at which such internal drainage ceases is known as the *field capacity*.

(ii) **Maximum Retentive Capacity** : During the course of a heavy rain or irrigation the soil might get saturated with water causing instant downward drainage. This saturation point with respect to water is known as the soil's *maximum retentive capacity*.

(iii) **Permanent Wilting Percentage** : As the soil dries up, plants begin to wilt during daytime in the presence of high temperatures and wind movement. Initially, the plants regain their vigour at night. A time comes when the rate of supply of water is so low that the plants remain wilted night and day. The moisture content of the soil at this stage is called the *permanent wilting percentage*.

(iv) **Hygroscopic Coefficient** : If a soil is kept in an atmosphere completely saturated with water vapor (98% relative humidity), it loses the liquid water held even in the smallest of micropores. The remaining water remains associated with soil particle surfaces as adsorbed moisture. It is held so tightly that much of it is considered non liquid and can move only in the vapor phase. The soil moisture content at this point is known as the *hygroscopic coefficient*.

CHAPTER III

REVIEW OF LITERATURE

Over the past two decades, a number of studies have been carried out to determine the dielectric behaviour of soil-water mixtures (Wiebe, 1971; Leschanskii et al., 1971; Poe, 1971; Geiger and Williams, 1972; Hipp, 1974; Hoekstra and Delaney, 1974; Newton and McClellan, 1975; Davis et al., 1976; Wobschall, 1977; Wang et al., 1978; Wang, 1980; Wang and Schmugge, 1980; Shutko and Reutov, 1982; Dobson et al., 1985; Hallikainen et al., 1985; Jackson and Schmugge, 1989; Narasimha Rao et al., 1990; Jackson, 1990; Scott and Smith, 1992; Alex and Behari, 1996).

A WET SOIL MEDIUM is a mixture of soil particles, air voids and liquid water. The liquid water contained in the soil is usually divided into two fractions : i) bound water and, ii) free water. Bound water refers to the water molecules contained in the first few molecular layers surrounding the soil particles; these are tightly held by the soil particles due to the influence of the matric and osmotic forces (Baver, L.D. et al., 1977).

Because the matric forces acting on a water molecule decrease rapidly with distance away from the soil particle surface, water molecules located several molecular layers

away from soil particles are able to move within the soil medium with relative ease, and hence are referred to as "free". Dividing the water into bound and free fractions describes only approximately the actual distribution of water molecules within the soil medium and is based on a somewhat arbitrary criterion for the transition point between bound and free water layers. The amount of water contained in the first molecular layer adjoining the soil particles is directly proportional to the total surface area of the soil particles contained in a unit volume. The total surface area of the particles is, in turn, a function of the soil particle-size distribution and mineralogy. A soil usually is assigned to a textural class on the basis of its particle-size distribution (Leschanskii et al., 1971).

Electromagnetically, a soil medium is a four-component dielectric mixture consisting of air, bulk soil, bound water, and free water. Due to the high intensity of the forces acting upon it, a bound water molecule interacts with an incident electromagnetic wave in a manner dissimilar to that of a free water molecule, thereby exhibiting a dielectric dispersion spectrum that is very different from that of free water. The complex dielectric constants of bound water and free water are each a function of the e.m. frequency f, the physical temperature 'T', and the salinity

'S'. Soil mixture is, in general, a function of : (i) f, T, S, (ii) the total volumetric moisture m_v, (iii) the relative fractions of bound and free water, which are related to the soil surface area per unit volume, (iv) the bulk soil density, (v) the shape of the soil particles, and (vi) the shape of the water inclusions (Hallikainen et al., 1985).

I. BULK DENSITY EFFECTS:

Soil moisture content is commonly expressed in gravimetric or volumetric units. Electromagnetically, the volumetric unit is preferred because the dielectric constant of the soil-water mixture is a function of the volume fraction in the mixture. This preference is evident in the plot shown in Fig 3.1 and 3.2, in which a greater degree of scattering about the regression curve is apparent of the plots of ε' and ε'' vs m_g than those plotted vs m_v (Lundien, 1971; Hallikainen et al., 1985).

II. MOISTURE, TEXTURE AND FREQUENCY DEPENDENCE :

In order to understand the effect of texture on the dielectric permittivity of soil, we consider the behaviour of water as it is added to a dry soil sample. Liquid water has a high dielectric constant due to the ability of its molecules to align their dipole moments along an applied field. Because of this, any phenomenon which hinders molecular rotation (eg., freezing, very high frequencies,

Soil Dielectric Constant, ϵ'_{soil}

$\rho_b = 1.6\, g\, cm^{-3}$ $\rho_b = 1.2\, g\, cm^{-3}$

m_v

m_v

Soil: Openwood Street Silt
Frequency: 1.074 GHz

Compaction ($N\, cm^{-2}$)	Moisture By	
	Volume	Weight
5.74	●	o
11.83	▼	Δ
18.47	■	□

Volumetric Moisture Content, m_v ($g\, cm^{-3}$)

Gravimetric Moisture Content, m_g (% by Weight)
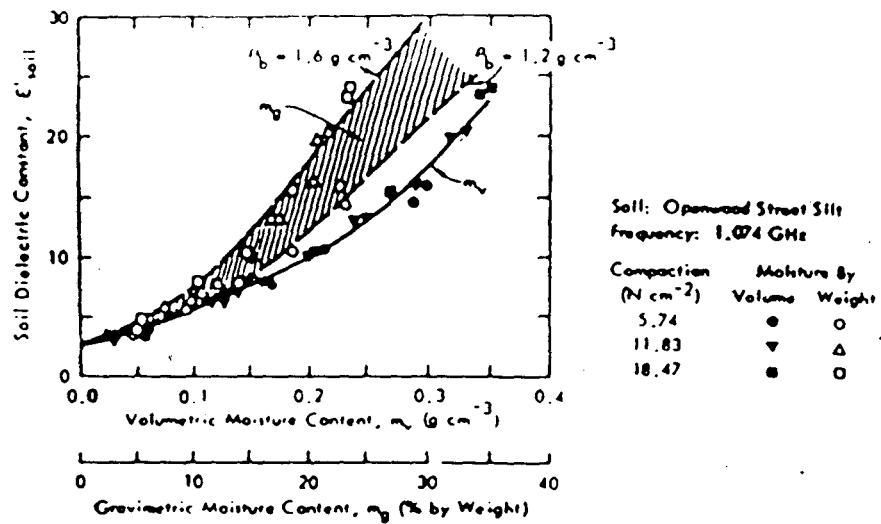
Fig 3.1: Variation in the relative dielectric constant due to soil-moisture units (from Cihlar and Ulaby, 1974; based on data from Lundien, 1971)

Field 1: Sandy Loam
Frequency: 5 GHz

ϵ'_{soil}

Dielectric Constant ϵ_{soil}

Point	ρ_b
1	1.18 $g\, cm^{-3}$
2	1.72 $g\, cm^{-3}$

ϵ''_{soil}

Field 1: Sandy Loam
Frequency: 5 GHz

ϵ'_{soil}

ϵ''_{soil}

Gravimetric Moisture m_g (%)

Volumetric Moisture m_v

Fig. 3.2: Comparison of ϵ'_{soil} and ϵ''_{soil} plotted as a function of (a) gravimetric moisture and (b) volumetric moisture (from Hallikainen et al., 1985).

tight binding to a soil particle) will reduce the dielectric constant of water. The first water molecules which are added to the soil are tightly bound to the soil particle surface and contribute only a small increase to the soil's dielectric constant. With addition of more water beyond some transition level W_T, the additional molecules (which are farther away from the particle surface and are free to rotate) make a larger contribution to the soil's dielectric constant. The surface area of soils depend upon their texture. Clay soils with larger surface area are able to hold more of this tightly bound water than sandy soils. As a result, the transition point W_T, occurs at a higher moisture level in clay then in sandy soils (Schmugge, 1983).
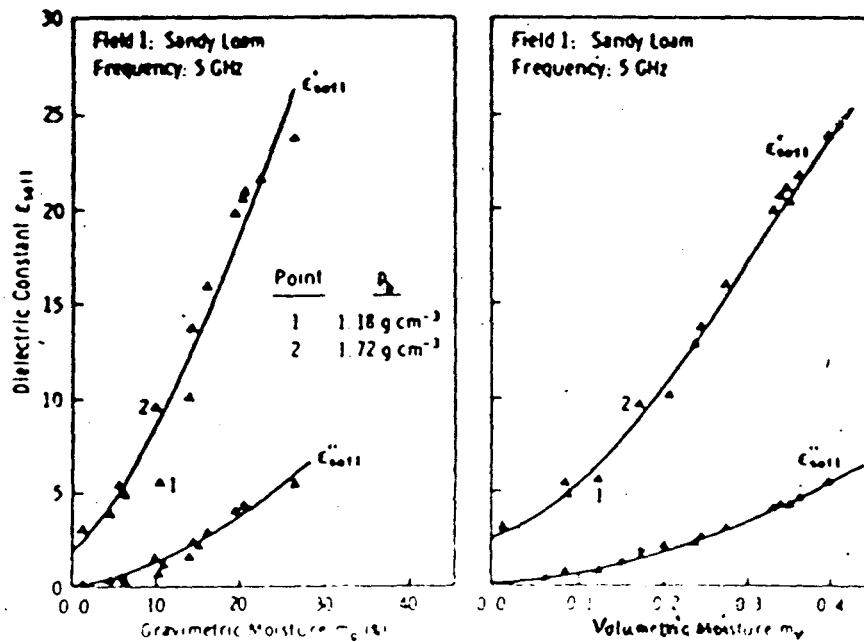
The above observations are supported closely by experimental results (Schmugge, 1983; Hallikainen et al., 1985). Figs. 3.3, 3.4, 3.5 and 3.6 show the moisture dependence of dielectric constant at different frequencies. At each frequency all the curves for ϵ' and ϵ'' have almost the same intercept at m_v = o showing little textural dependence for dry soils. The plots exhibit the same general shape but have different curvatures for different texture types. At any given moisture content and at all given frequencies, ϵ' was found to be roughly proportional to the sand content. The effect of soil texture was found

Field	Soil Type	Sand (%)	Silt (%)	Clay (%)
1	Sandy Loam	51.5	35.0	13.5
2	Loam	42.0	49.5	8.5
3	Silt Loam	30.6	55.9	13.5
4	Silt Loam	17.2	63.8	19.0
5	Silty Clay	5.0	47.6	47.4

Frequency: 1.4 GHz
T = 23°C

Dielectric Constant ε_{soil}

ε'_{soil}

ε''_{soil}

Volumetric Moisture m_v
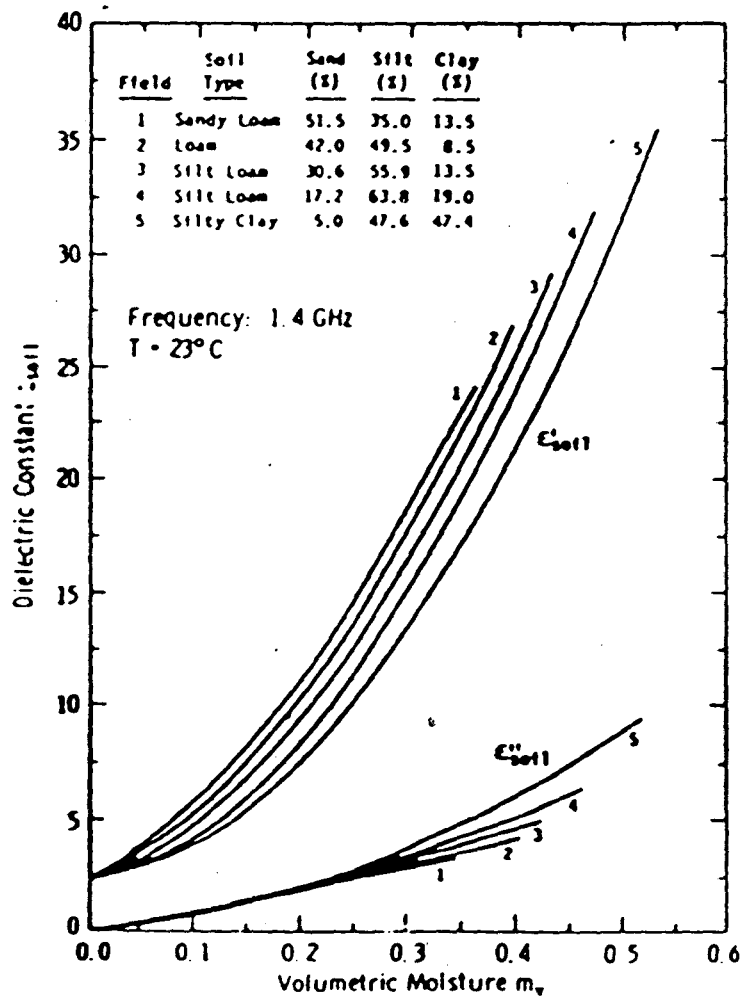
Fig. 3.3: Measured ε'_{soil} and ε''_{soil} for different textural classes at 1.4 GHz. (from Hallikainen et al., 1985).
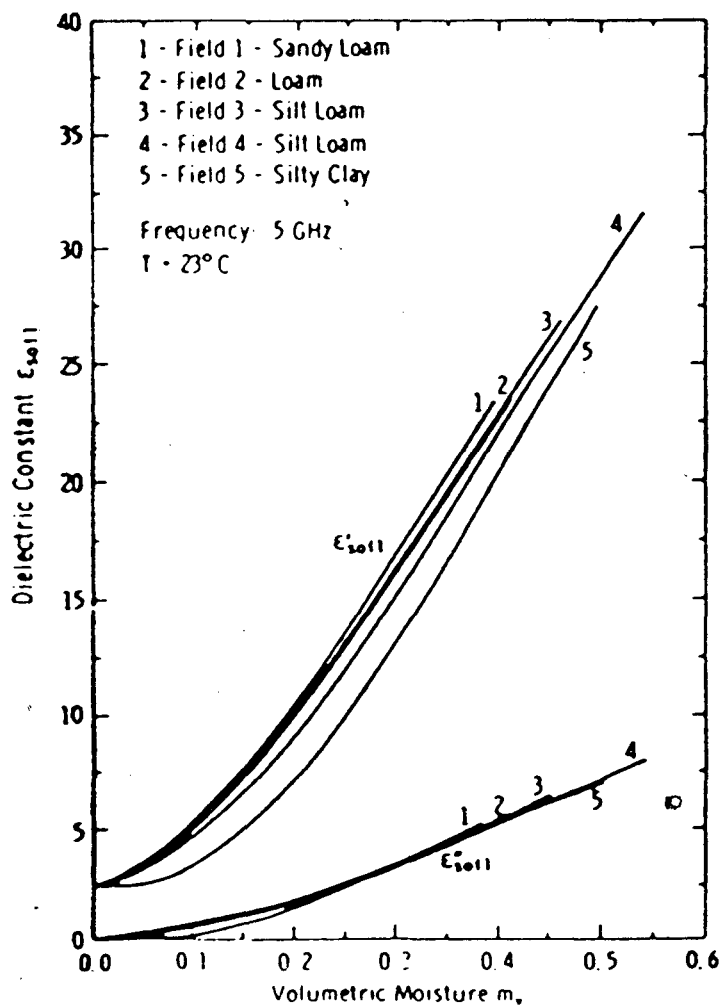
Fig. 3.4: Measured ε'_{soil} and ε''_{soil} for different textures at 5 GHz. (from Hallikainen et al., 1985).
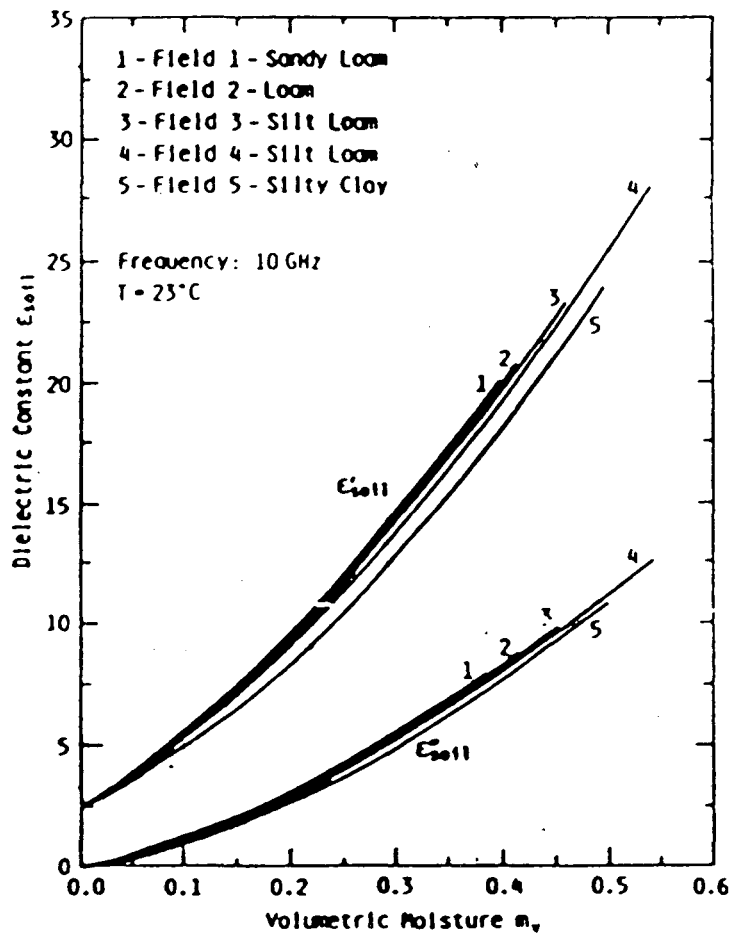
Fig. 3.5: Measured ε'_{soil} and ε''_{soil} for different textures at 10 GHz (from Hallikainen et al., 1985)
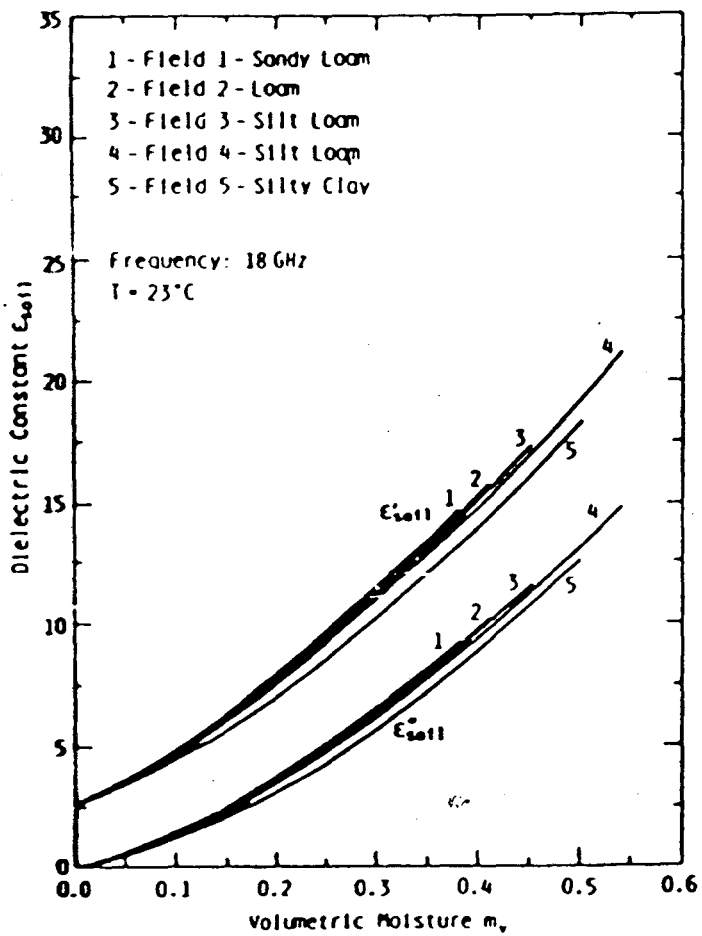
Fig. 3.6: Measured ε'_{soil} and ε''_{soil} for different textures at 18 GHz (from Hallikainen et al., 1985).

to decrease with frequency. The effect of texture on the loss factor is more complicated. At 1.4 GHz ϵ'' was seen to increase with soil clay content. At 4.0 to 6.0 GHz, ϵ'' is nearly independent of soil texture at all moisture conditions. At frequencies of 8.0 GHZ and above, ϵ'' was observed to decrease with soil clay fraction; further more, the magnitude of this behaviour increases with frequency.

Hoekstra and Delaney (1974) in their studies carried out measurements of complex dielectric constant of four soil types in the frequency range o.1 to 26 GHz. Their results showing the special variation of ϵ' (soil) is depicted in fig. 3.7. for two volumetric moisture contents.

In a later study, Hallikainen and others (1985) measured ϵ' for several soil types. A portion of their results is shown in fig 3.8. It shows dependence of ϵ'_{soil} (m_v) on frequency. Their measurements were carried out at 23°c. At this temperature the relaxation frequency of water is 18.6 GHz. It was reported that the real part of the dielectric constant reduced with increasing frequency.

In a more recent study, Alex and Behari (1996) also reported that in case of dry soils the dielectric parameters are not very sensitive to soil texture. However, for wet soils (m_v > 0.2) the dielectric parameters are significantly dependent upon the soil texture. A subset of their results
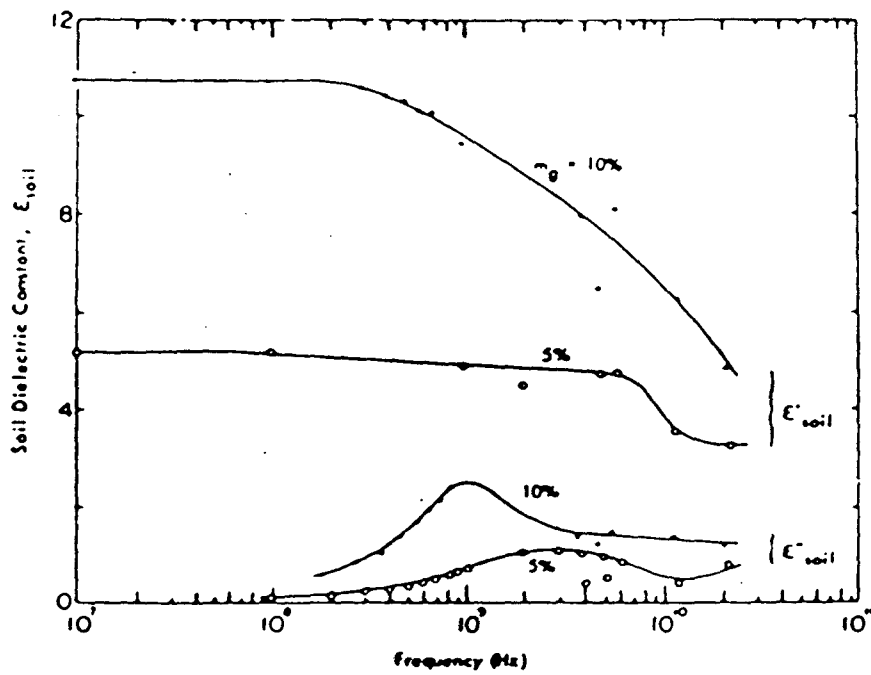
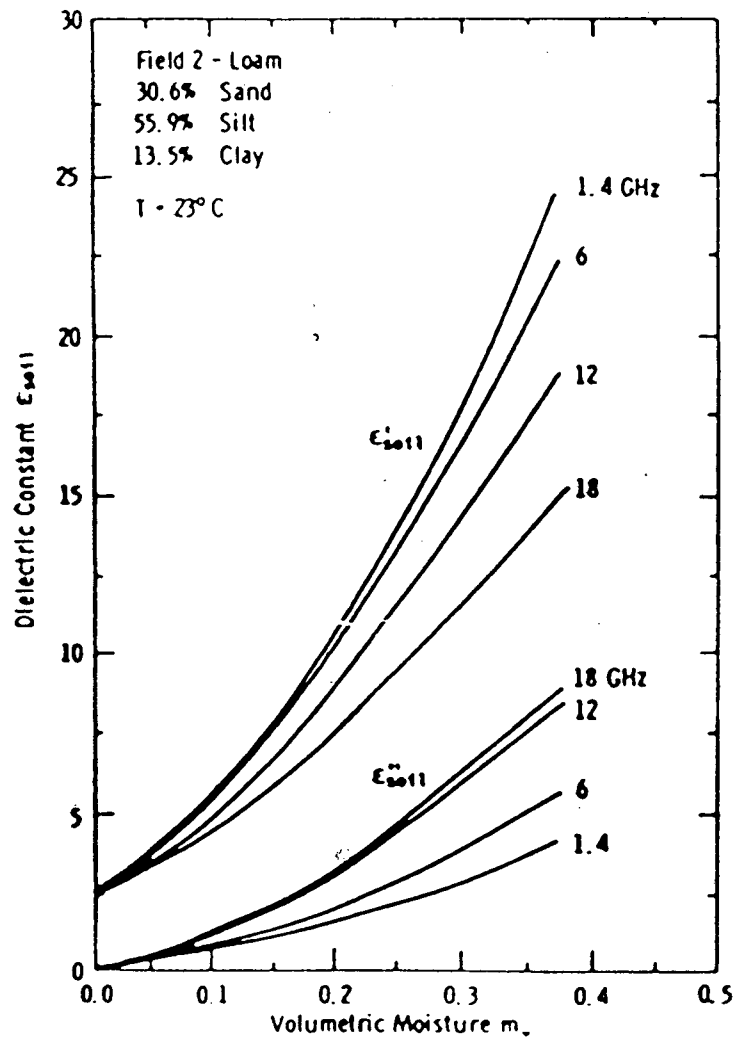Fig. 3.7: Variation of ε' and ε" of a clayey soil with frequency (from Hoekstra and Delaney, 1974).

Fig. 3.8: Dependence of ε'_{soil} and ε''_{soil} with the measuring frequency (from Hallikainen et al., 1985)

are shown in fig 3.9 and 3.10. In the reported frequency range(0.6 - 1.2 GHz), they found that the frequency variation of the dielectric constant is not significant for dry soils but quite prominent for wet soils. This clearly indicates that this is due to the effect of moisture content and the corresponding density variation.

III. TEMPERATURE DEPENDENCE :

The temperature dependence of ϵ' is shown in fig 3.11 for a clay soil at 10 GHz. It is observed that above 0°C, ϵ'_{soil} and ϵ''_{soil} exhibit a much weaker dependence on frequency compared to their dependence at temperatures below 0°C. The same conclusion was also reached by Poe et al. (1971) and by Davis et al., (1976). Hallikainen et al. (1985) also studied the temperature dependence. Figs.3.12 and 3.13 illustrate that at temperatures well below freezing point (0°C), ϵ' and ϵ'' exhibit a much weaker dependence on frequency compared to their dependence at temperatures above freezing point (0°C). In the absence of liquid water, frozen soil is a mixture of air (permittivity : 1), soil solids with permittivity approx. 3.15. Hence, in view of the relative high volumetric water contents of the sample represented in fig 3.11, one would expect ϵ' of the mixture to be around 4 at below freezing temperatures. This is consistent with the level of the - 50° C curves.
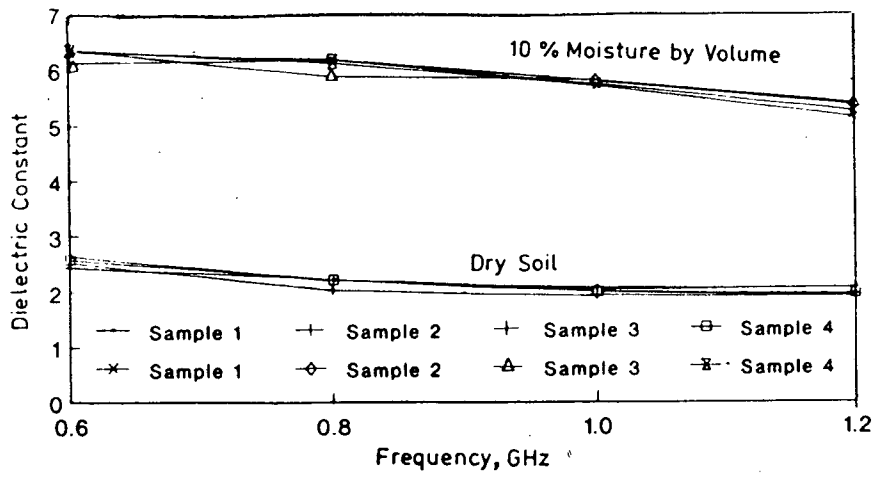
Fig. 3.9: Dependence of dielectric constant on frequency texture and moisture (from Alex and Behari., 1996).
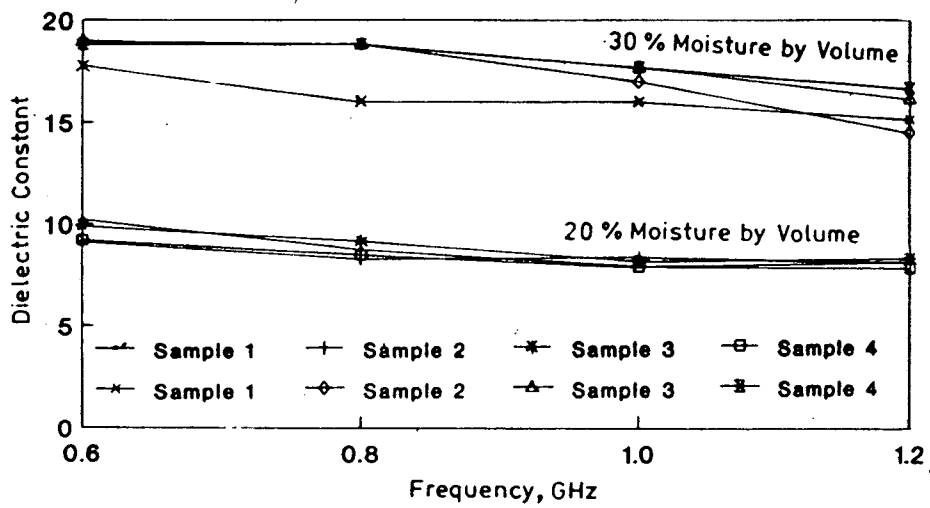
Fig 3.10: Dependence of dielectric constant on frequency texture and moisture (from Alex and Behari., 1996).
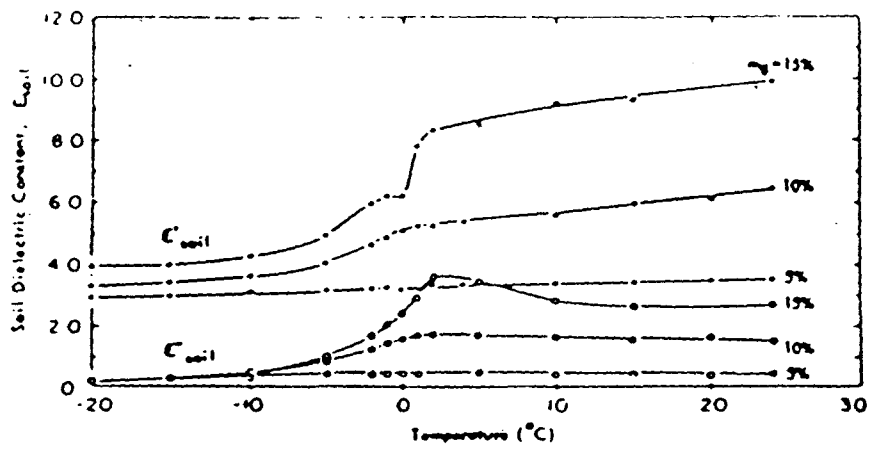
Fig. 3.11: Dielectric constant of a clayey soil as a function of temperature at 10 GHz. (from Hoekstra and Delaney, 1974).

Temperature:
+23° • -2°
+10° • -10°
+2° • -25°
• -50°

Field 1 - Sandy Loam
$m_v = 0.24$

(a)

Field 3 - Silt Loam
$m_v = 0.26$

(b)

Field 5 - Silty Clay
$m_v = 0.24$

Dielectric Loss Factor ε''_{soil}
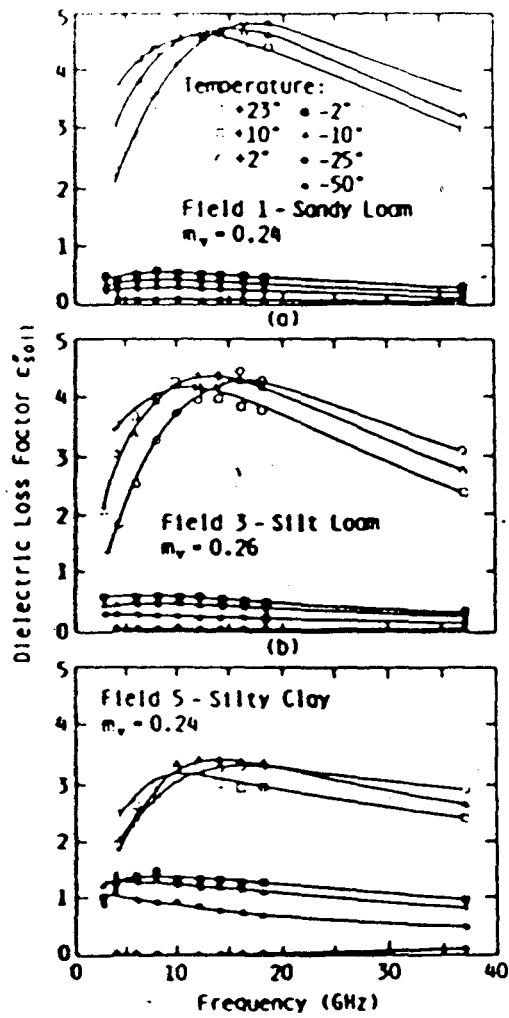
Frequency (GHz)

Fig. 3.12: Permittivity of soils as a function of frequency and temperature.
(Hallikainen et al., 1984).
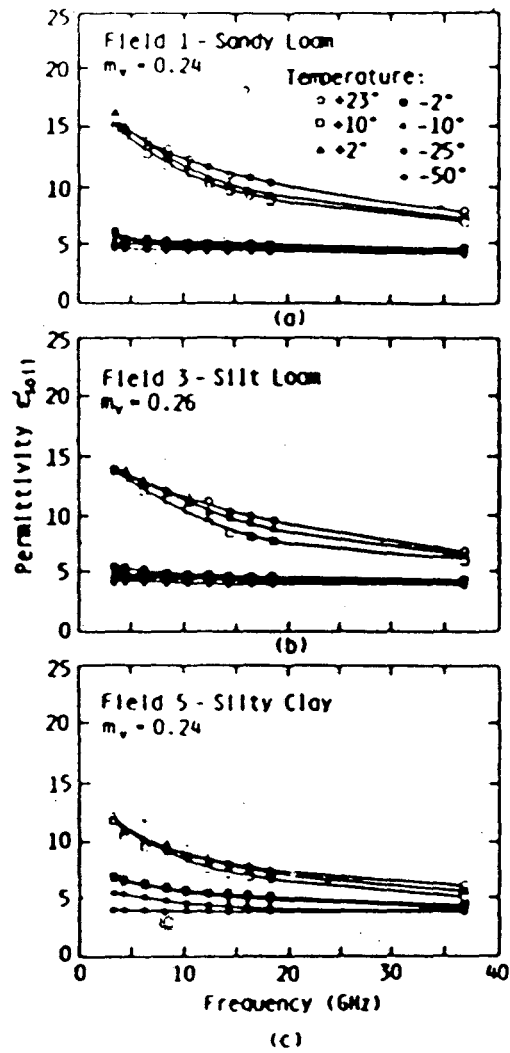
Fig. 3.13: Loss factor of soils as a function of frequency and temperature.
(Hallikainen et al., 1984)

IV. SALINITY DEPENDENCE:.

Below 10 GHz, the ionic conductivity of saline water may have a marked effect on the loss factor ϵ''. Consequently high soil salinity may significantly influence the dielectric properties of wet soil. The exact form of dependence of ϵ_{soil} on salinity is, however not well understood.

V. DEPENDENCE OF REFLECTIVITY ON MOISTURE CONTENT AND PERCENT FIELD CAPACITY (ELIMINATION OF TEXTURE EFFECT):

In a recent study for elimination of textural effects in microwave remote sensing of soil moisture (Narasimha Rao et al., 1990), the soil moisture was expressed in terms of gravimetric (M_g) and volumetric (M_v) units and the percent field capacity (M_{fc}). These were then plotted individually against the reflectivity at 4.75 GHz. (Figs.3.14, 3.15, 3.16). From fig 3.15 it can be seen that when soil moisture is in M_v, the textural effects are significantly reduced as compared to when they are expressed in M_g or M_{fc}. When the soil moisture is in M_{fc}, the effect due to sandy loam and silt loam soils has been eliminated. However, it was noted from figs.3.14 and 3.16 that the relative position of curves belonging to sandy loam and silty clay soils had got interchanged, leading to over compensation of the texture effect, which is in agreement with Dobson et al., (1984).

29
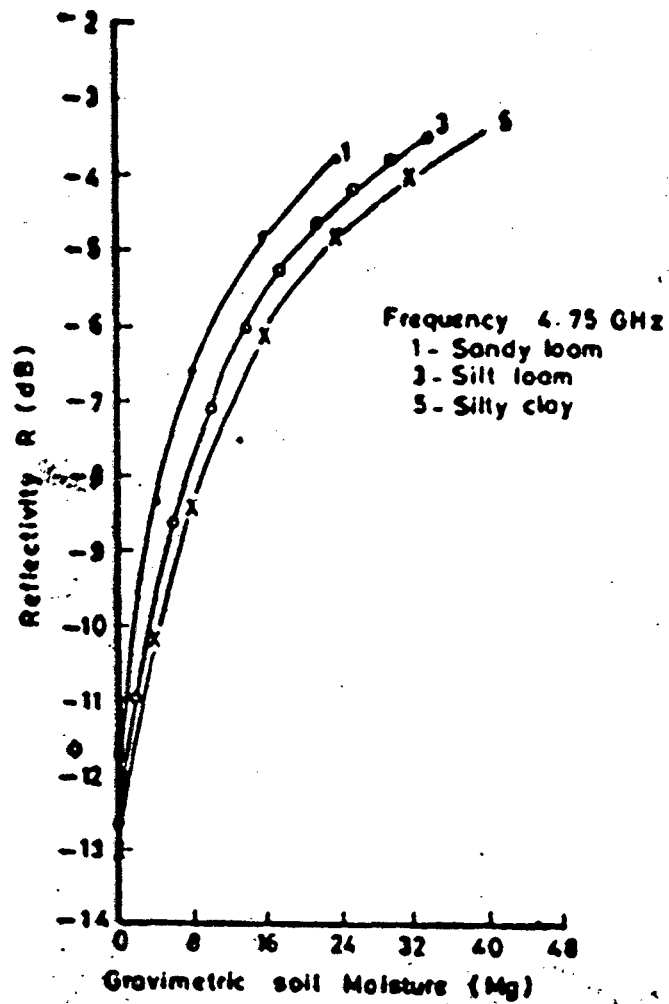
Fig. 3.14: Reflectivity of three soils as a function of moisture content expressed in gravimetric units. (from Narasimha Rao et al., 1990).
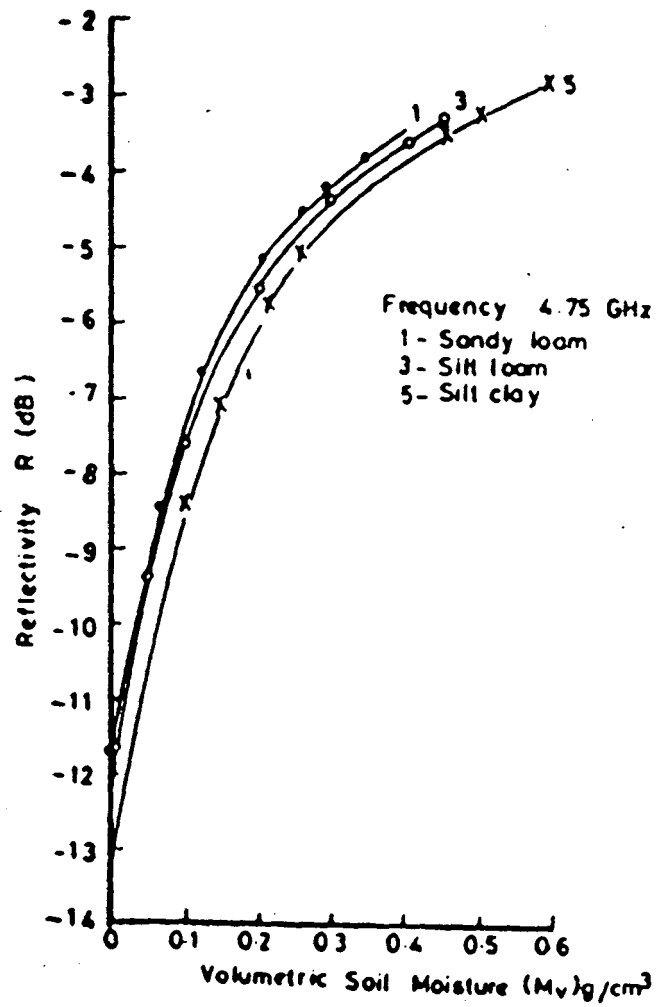
Fig. 3.15: Reflectivity of three soils as a function of moisture content expressed in volumetric units (from Narasimha Rao et al., 1990).
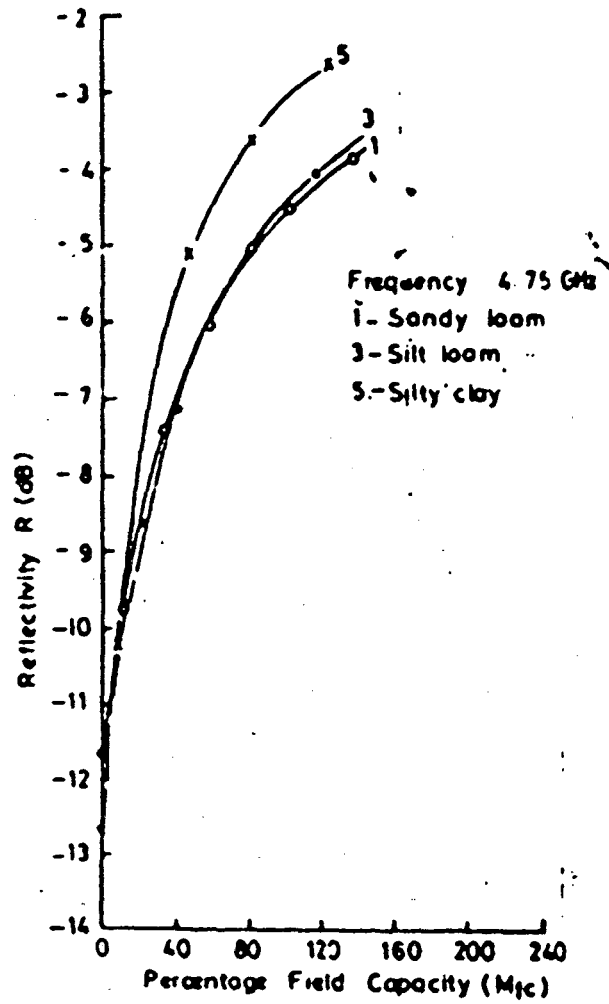
Fig. 3.16: Reflectivity of three soils as a function of moisture content expressed percent of field capacity (from Narasimha Rao et al., 1990).

MODELS :

There have been several attempts to model the microwave dielectric behaviour of soil water mixtures, ranging in complexity from a simple two-component formula to elaborate physical soil models. Shutko and Reutov (1982) evaluated several two-component formulas one of which is :

$$\epsilon_m^{\alpha} = \epsilon_n^{\alpha} + v_i \ (\epsilon_i^{\alpha} - \epsilon_n^{\alpha}) \qquad \ldots \ (3.1)$$

here, ϵ_m is the dielectric constant of the mixture,

ϵ_n is the dielectric constant of the host material,

ϵ_i is the dielectric constant of inclusions,

v_i is the volume fraction of inclusions.

Eq. 3.1 with $\alpha = 1/2$, may be used as a working model. A two-component (Soil plus water) model can, at best, exhibit the correct trend for ϵ_{soil} vs m_v, but cannot account for the dependence on soil type. More elaborate models have been proposed (Hoekstra and Delaney, 1974; Wobschall, 1977; Wang, 1980), which implicitly or explicitly recognize the importance of bound water in the overall dielectric behaviour of the mixture. It is possible to obtain better agreement between measured data and these models than is possible with two-component models, but this is in part because the more elaborate formula include adjustable soil-specific or frequency-specific parameters.

WANG AND SCHMUGGE MODEL

Wang and Schmugge (1980) have offered an empirical mixing formula at 1.4 and 5 GHz that explicitly treats a bound water layer and an air volume fraction in addition to the dry soil and bulk water components. In their treatment the complex dielectric constant components are linearly combined over two separate regions :

(i) for water components $W_c \leq$ the maximum bound water (transition moisture W_t) fraction, and

(ii) for water contents $W_c >$ the bound water (transition moisture W_t) fraction

The expression for the complex dielectric constants (of a soil - water mixture) in this model is :

$$\epsilon = W_c \, \epsilon_x + (P - W_c) \, \epsilon_a + (1-P) \, \epsilon_r; \quad W_c \leq W_t \quad \ldots \quad (3.2)$$

$$\text{with } \epsilon_x = \epsilon_i + (\epsilon_w - \epsilon_i) \, W_c/W_t \cdot \gamma \quad \ldots \quad (3.3)$$

and,

$$\epsilon = W_t \, \epsilon_x + (W_c - W_t) \, \epsilon_w + (P - W_c) \, \epsilon_a + (1-P) \, \epsilon_r; \quad W_c > W_t \quad \ldots \quad (3.4)$$

$$\text{with } \epsilon_x = \epsilon_i + (\epsilon_w - \epsilon_i) \gamma \quad \ldots \quad (3.5)$$

here P is the porosity of dry soil given by,

$$P = 1 - \rho_s/\rho_r$$

where, ρ_s is the density of dry soil and, ρ_r is the density of the associated solid rock. ϵ_a, ϵ_w, ϵ_r and ϵ_i are the

dielectric constants of air, water, rock and ice respectively and ϵ_x is the dielectric constant of the initially absorbed water. γ is a parameter which can be chosen to best fit eq. (3.2) and (3.4) to the experimental data. For the soil samples used in the dielectric measurements at 2.4 and 5 GHz, ρ_s lies in the range of 1.1 - 1.7 g/cm^3, while ρ_r varies between 2.6 - 2.75 g/cm^3. Entering the average value of ρ_s for the soil samples in eq.(3.6) gives P = 0.5. It can be shown that with either P = 0.4 or P = 0.6, the calculated dielectric constants of a soil-water mixture differ only slightly from those with P= 0.5. The dielectric constants of ice, (real and imaginary) are assumed to be approximately 3.2 and 0.1 respectively and frequency independent at a frequency of 1 GHZ (Evans, 1965). The dielectric constants (real and imaginary) of a solid rock vary (Campbell, 1969) but the respective values of 5.5 and 0.2 fit well with the experimental value of dry soils.

With the Wang and Schmugge (1980) model, the values of transition moisture W_t, and W_p were determined for 18 soils by a least square fit to the experimental data. The value of W_t and W_p can also be obtained from the set of expression given below.

W_p = 0.068 - 0.00064sand + 0.0048 clay   ... (3.7)

producing the following relation,

$$W_t = 0.49 \, W_p + 0.016 \qquad \ldots (3.8)$$

$$\text{and,} \quad \gamma = -0.57 \, W_p + 0.48 \qquad \ldots (3.9)$$

The correlation coefficient for W_t is 0.9 and for W_p it is 0.8 indicating that there is a strong dependence on W_p and that the texture data can be used to estimate the value of W_t for a soil. For the imaginary part of the dielectric constant at low frequencies it is necessary to add a conductivity loss and the total dielectric loss ϵ_t'' becomes

$$\epsilon_t'' = \epsilon'' + \epsilon_\sigma''$$

$$= \epsilon'' + 60 \, \lambda \, \sigma$$

$$= \epsilon'' + \alpha W_c^2 \qquad \ldots (3.10).$$

where the conductivity loss ϵ_σ'' is assumed to be proportional to W_c^2 based on the data of soil (Wang and Schmugge, 1980). σ is the ionic conductivity in mhos/cm and λ is the wavelength (cm). ϵ'' represents the imaginary part of the mixed dielectric constant formed from pure water and dry soil as obtained from eq. (2.2) and (2.4). α is the parameter chosen to best fit the measured ϵ_t''

The above mixing model does not consistently predict the measured behaviors of the imaginary part of the dielectric constant. The model demonstrates the importance of considering the bound-water volume as a distinct dielectric constituent of the soil-water system and indicates that the effective conductivity loss is dependent

upon both soil type and water content. Also the model shows that both the bound-water fraction and the effective conductivity loss are positively correlated with clay content.

PHYSICAL SOIL MODEL

To eliminate the dependence upon adjustable parameters, Dobson et al., (1985) developed a physical soil model that is dependent upon measurable soil characteristics only and requires no adjustable parameters to fit experimentally measured data. This soil model apportions the soil solution into a bound water volume fraction and into a free water volume fraction, in accordance with the pore size distribution calculated from the particle size distribution. This model uses the multi phase formula for a mixture containing randomly oriented inclusions.

$$\epsilon_m = \epsilon_n + \frac{1}{3} \sum_{i=1}^{n} v_i (\epsilon_i - \epsilon_n) \sum_{u_i=a_i,b_i,c_i} [\frac{1}{1+A_{ui} (\epsilon/\epsilon^* -1)}]$$

$$\ldots (3.11)$$

The mixture contains solid soil as the host material and three types of inclusions, bound water, free water, and air, all of which are assumed to be disc-shaped and whose size is governed by the particle-size distribution and the total amount of water in the mixture. Examples of the calculated dielectric constants from the physical soil

model, ϵ_{calc}, are compared with the measured values, ϵ_{meas}, in fig 3.17 for sandy loam, silt loam and silty clay. In general, the predicted values closely follow the trends of the measured data for all soils tested at all frequencies between 1.4 and 18 GHz.

SEMI - EMPIRICAL MODEL

The data set referred to above in connection with the physical soil model was also used to develop a relatively simple semi - empirical model (Dobson et al., 1985). Eq. (3.12) can be written for a four - component mixture where the subscripts ss, a, fw and bw denote soil solids, air, free water and bound water respectively.

$$\epsilon_{soil} = V_{ss}\epsilon_{ss} + V_a\epsilon_a + V_{fw}\epsilon_{fw} + V_{bw}\epsilon_{bw} \qquad \cdots (3.12)$$

As noted earlier,

$$\epsilon_{ss} \simeq 4.7 - jo \qquad \cdots (3.13)$$

Also,

$$V_s = 1 - V_\phi$$

$$V_a = V_\phi - m_v$$

$$m_v = V_{fw} + V_{bw}$$

$$P = (\rho_{ss} - \rho_b)/\rho_{ss} \simeq 1 - 0.38\,\rho_b \qquad \cdots (3.14)$$

Where P is the soil porosity. $\rho_{ss} \simeq 2.65$ gm/cm^3 is the density of the solid soil material, and m_v is the total volumetric moisture content. To simplify (3.12) and yet retain some dependence on soil textural composition, the
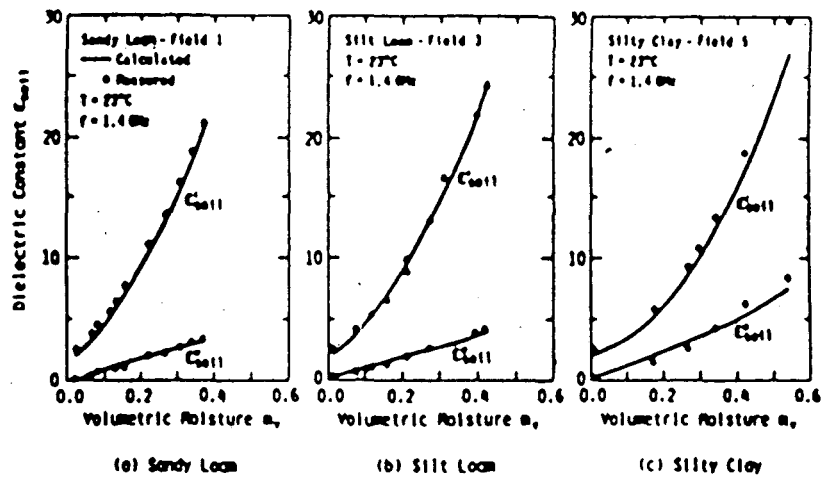
Fig. 3.17: Comparison of ε' and ε" values predicted by the physical soil model with measured values at 1.4 GHz for three soil types (for textural composition please refer fig. 3.3 ; Hallikainen et al., 1985)

last two terms were combined into a single term,

$$V_{fw} \, \epsilon_{fw}^{\alpha} + V_{bw} \, \epsilon_{bw}^{\alpha} \simeq m_v^{\beta} \, \epsilon_{fw}^{\alpha} \qquad \ldots \ (3.15)$$

Where ß is an adjustable parameter to be determined empirically.

Incorporating the above equations,

$$\epsilon_{soil} = (1-V_\phi) \, \epsilon_{ss}^{\alpha} + V_\phi - m_v + m_v^{\beta} \, \epsilon_{fw}^{\alpha}$$

$$= 1 + \frac{\rho_b}{\rho_{ss}} \, (\epsilon_{ss}^{\alpha} - 1) + (m_v^{\beta}\epsilon_{fw}^{\alpha} - m_v)$$

$$\simeq 1 + \frac{\rho_b}{\rho_{ss}} \, (\epsilon_{ss}^{\alpha} - 1) + m_v^{\beta} \, (\epsilon_{fw}^{\alpha} - 1) \qquad \ldots \ (3.16)$$

As we will see below, ß was found to vary between approximately 1.0 and 1.16 for the five soil types used in the investigation (result inset in fig 3.3 for textural composition). This is the justification for approximating m_v as m_v^{β} in the last term in eq. 3.16. If we limit the model to frequencies higher than 4 GHz, the effects of soil salinity may be ignored. The dielectric constant of pure water at 23°C is,

$$\epsilon_{fw} = 4.9 + \frac{74.1}{1+j \ (f/f_o)} \qquad \text{-----------}(3.17)$$

Where f_o = 18.64 GHz is the relaxation frequency of water.

The data set used by Dobson et al., (1985) contained over 500 data points distributed approximately equally among

five soil types, & consisted of dielectric measurements at nine frequencies extending between 4.0 GHz and 18 GHz for volumetric moisture between $m_v = 0.01$ and saturation. For each soil type, the data was fitted to eq.(3.16) to determine the values of α and β that yield minimum rms difference between the values of ϵ'_{soil} and ϵ''_{soil} provided by the model and those measured experimentally. The value $\alpha=0.65$ was found to be optimum for all soil types; the magnitude of β was found to vary from about 1.0 for sandy soil to 1.17 for silty clay, and can be related to the sand (s) and clay (c) fraction (by weight) of the soil, as,

$$\beta = 1.09 - 0.11s + 0.18c \qquad \ldots (3.18)$$

with a multiple correlation coefficient $r^2 = 0.96$. In a perfect model, a simple linear regression of the calculated values of ϵ against the measured data ϵ_{meas} would produce a relationship with a zero intercept, a slope of unity, and a correlation coefficient r^2 close to unity. The scatter plot shown in fig (3.18) is a typical example of the model performance for ϵ_{soil}. In spite of the wide textural variety of the soil represented in fig. 3.13 excellent agreement is obtained between the calculated and measured values of ϵ'_{soil}. Similar results are obtained for ϵ''_{soil} (fig.3.19).
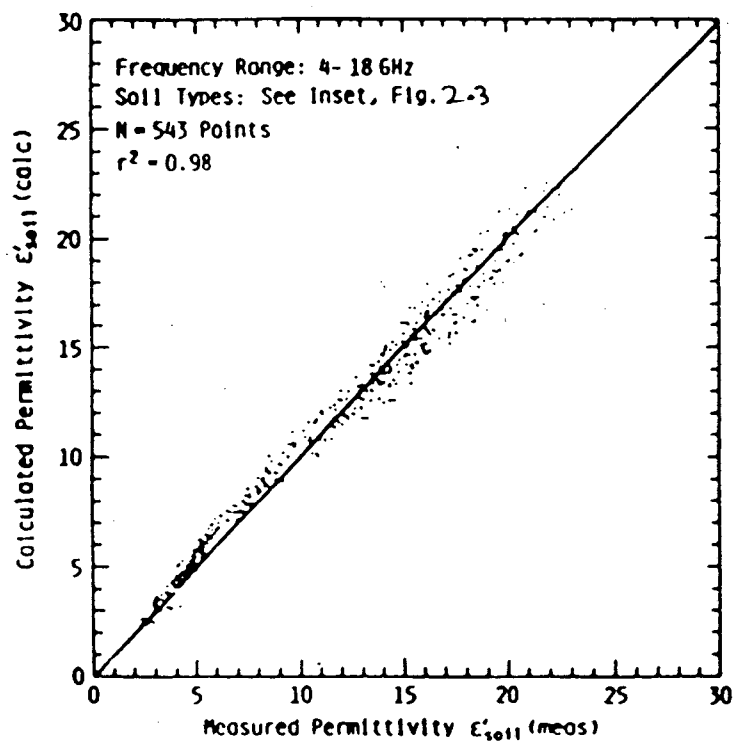
Fig. 3.18: Scatter diag. comparing ε'calc using eq. 3.16 with ε'meas
(from Dobson et al., 1985).

Fig. 3.19: Scatter diag. comparing s"calc using eq. 3.16 with s"meas
(from Dobson et al., 1985).

A RECENT STUDY

In their recent studies, Alex and Behari (1996) had put forward an empirical model for calculation of the volumetric soil moisture from the real part of the complex dielectric permittivity of the soil sample.

Their proposed model consists of two steps. In the first step, the emissivity `e' of the soil sample is calculated by a known formula using just the real part of the complex dielectric constant ϵ':

$$e = 1 - \left| \frac{1 - \sqrt{\epsilon'}}{1 + \sqrt{\epsilon'}} \right|^2 \qquad \ldots (3.19)$$

In the next step. The volumetric soil moisture (m_V) is calculated using a second formula involving 'e'.

$$m_V (\%) = -0.8317 \, e^{-2} + 2.793 \, e^{-1} - 2.04 \qquad \ldots (3.20)$$

Although this model is yet to gain acclaim from all quarters, it provides a direct method of calculating the soil moisture content directly by the knowledge of the microwave dielectric permittivity and has potential to transform into an useful tool in insitu soil moisture measurements.

CHAPTER IV

EXPERIMENTAL TECHNIQUES

A variety of experimental procedures for determination of the dielectric parameters of various samples of differing size and shape have been summarised by different authors (Von Hippel, 1961; Montgomery, 1961; Sucher et al., 1963; Musil et al,. 1986; Roberts et al., 1946; Brunfeldt, 1987; Dalton et al., 1986; Buck master et al., 1985; to mention a few).

These different measurement techniques can be broadly classified into two categories:

(1)   Time domain techniques, and

(2)   Frequency domain techniques

Of there two classes, the Time Domain technique is of a more recent origin.   It has been employed by several investigators for the dielectric properties as well as moisture content measurement of soils (Topp et al., 1980; Dalton et al., 1986).   Especially popular in this class of techniques is the Time Domain Reflectometry (TDR) method. In Time Domain techniques the permittivity of the sample is calculated from the measured resonance frequency and q-factor resonant methods.

The Frequency Domain techniques can be further classified into the following subgroups:

(i) Free Space Technique

(ii) Cavity Perturbation Techniques (Sucher et al., 1963; Musil et al., 1986)

(iii) Transmission Techniques in Wave Guides/coaxial lines, and

(iv) Reflection Techniques in Wave Guides/coaxial lines.

Free Space Technique :

This method is suitable for the measurement of permittivity of medium and high loss materials. This method is employed when two different purely reactive terminations of a sample are available. Suber and Crounch (1948) developed a method where the sample is enclosed within a section for which the wave ratio are measured for both short circuit and open circuit and $V_\epsilon = Y_{i1} \times Y_{i2}$ where Y_{i1} and Y_{i2} are the corresponding measured impedance. The greatest advantage of this method is that it is relatively simpler and does not involve solution of a transcendental equation.

Cavity Perturbation Techniques :

The method is in vogue for measurement of dielectric constants of low loss samples of small quantity which can be put into any convenient form. Measurement are recorded for two situations; cavity without sample and cavity with sample. The difference between these two manifest itself in

a small difference in the observed complex frequency (real frequency + Q factor). This is then used to calculate the dielectric constant of the sample. The method has been successfully employed by many investigators, (Bethe et al., 1943; Birenbaum et al., 1969; Aruna and Behari, 1981; Behari et al.,1982; Bayser et al., 1992; Boifot et al., 1992).

Transmission Techniques in Wave Guides/Coaxial Lines :

This method is particularly suitable for high loss samples. In such cases measurement is based on infinite sample length (when most of the energy entering the sample gets absorbed, the sample is termed as an infinite sample).

The normalized input impedance at the interface of two dielectrics, when the second one is of infinite length, is directly related to the dielectric properties of the two. In a wave guide with (TE_{10}) mode, the relative complex dielectric constant is,

$$\epsilon = \frac{1}{1 + (\lambda c/\lambda_g)^2} + \frac{1}{1 + (\lambda g/\lambda_c)^2} \left[\frac{\Gamma - j \tan\{k(D-D_R)\}}{1 - j \Gamma \tan\{k(D-D_R)\}} \right]$$

$$\ldots (4.1)$$

where, λ_g is the guide wavelength, and λ_c is the cut off wavelength, Γ is the VSWR and $(D-D_R)$ is the shift in minima position when an infinite sample is replaced with short circuit. A number of investigators have been successful

with this method (Behari et al., 1982; Bayser et al., 1992;
Boifot et al., 1992; Karolkar et al., 1985; to name á few).

Reflection Techniques in Coaxial lines/Wave Guides:

Reflection methods are usually adopted in a coaxial
line sample holder where the reflection coefficient or
scattering parameter are determined at a redefined reference
plane from the sample holder. The reflection coefficient
can be determined very easily with the use of a network
analyzer, using swept frequency technique or slotted line
apparatus or using a resonator terminated by the sample
(Stuchly et al., 1979, 1980). The resonator method uses an
infinite sample where changes in the resonating frequency
and Q factor produced by the sample are measured. For the
TEM mode, magnitude of the reflection coefficient is, $|\Gamma|$ =
exp $[-n \ (1/Q_\epsilon - 1/Q_O)]$ and phase angle $\theta = 2\pi n \ (1 - f_c/f_0)^n$
where resonance frequency with sample is f_c and resonating
frequency of the resonator without the sample is f_0. n is
dependent on resonator length $=(n_c/2l)$; the dielectric
parameter ϵ is given by

$$\epsilon_r = [\frac{1 - \Gamma}{1 + \Gamma}]^2 \qquad \qquad \ldots \ (4.2)$$

where $\Gamma = |\Gamma| \ e^{i\theta}$

42

This method can be applied for a lossy material with a high dielectric constant (eg: a biological tissue) but it is limited to a discrete frequency.

Resonator methods are not suitable for high loss liquids because the resonance peak becomes so broad that ϵ cannot be measured correctly. As an alternative, open cavity methods with high loss liquids filled in a capillary can be applied. A method has been devised by Van loon and Finsey (1975) involving computer analysis of the reflected power profile. The wave propagation constant is determined by fitting an analytical curve to the reflection profile, this then, yields the value of the complex permittivity.

In their recent investigations, Stabell and Misra (1990) designed a new procedure for in vivo dielectric measurement using an open ended line probe. Any system imperfection is completely bypassed in this method since the calibration is carried out with four materials of known dielectric constants and then the reflection coefficients of these materials are then used in the final calculations along with the reflection coefficient of the sample.

In case of reflection methods in wave guides, the reflection coefficient from a defined reference plane is put to use for permittivity measurements. The reflection coefficient itself may be measured by a slotted line or a

network analyzer or by simply forming a resonator terminated by the sample (Stuchly et al., 1978).

Two popular techniques involving measurement of reflection coefficient in a wave guide are :

(a) The Two Point Method and,

(b) The Single-horn Reflectometry Method. (Arcone et al., 1988)

Both these methods are suitable for either loss less dielectrics or dielectric with medium loss. These two methods have been adopted for measurement of soil complex permittivity at different moisture contents as part of the present work.

THE TWO POINT METHOD

The underlying theory of this method can be understood by a consideration of fig. 4.1 (a), which shows an empty short circuited waveguide with a probe located at a voltage minimum D_R. The next fig.4.1 (b) shows the same wave-guide, containing a sample length l_ϵ with the probe located at a new voltage minimum D. The sample is placed adjacent to the short circuit. Looking from $T_{\epsilon 1}$ towards the right and the left, one can write the impedance equation as.

$$Z_O \tan k_1 = -Z_\epsilon \tan k_\epsilon \, l_\epsilon \qquad \qquad \dots (4.3)$$

Similarly in fig 4.1 (a), looking toward the right, we have,

$$Z_O \tan k \, (l_R + l_\epsilon) = 0 \qquad \qquad \dots (4.4)$$
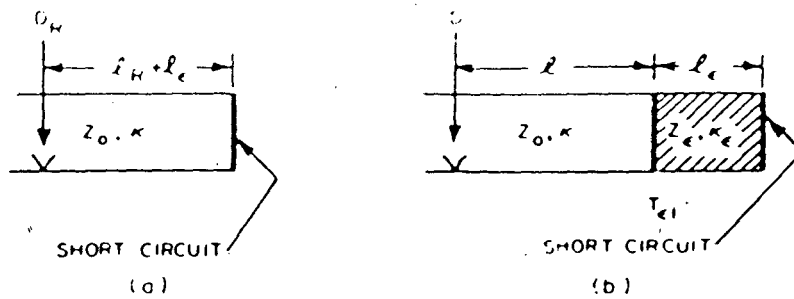
Fig. 4.1: Measurement of ε by the two point method (from Sucher and Fox, 1963)
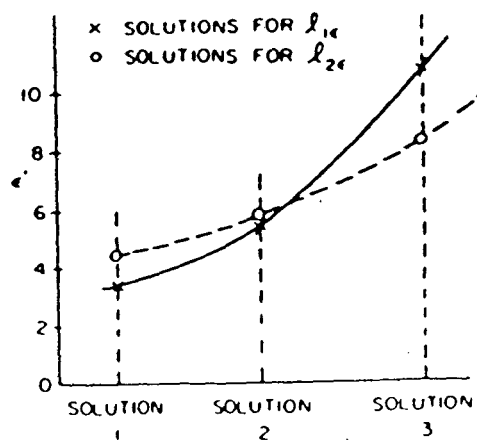
Fig. 4.2: Obtained solutions for ε' using two different sample lengths
(from Sucher and Fox , 1963)

Now,

$$\tan k\ (D_R - D + l_\epsilon) = \tan k[(l_R + l_\epsilon) - (1 + l_\epsilon) + l_\epsilon]$$

$$= \tan k[(l_R + l_\epsilon) - 1]$$

Expanding the tangent and using eq.(4.4) and substituting into eq.(4.3) we get,

$$Z_0 \tan k\ (D_R - D + l_\epsilon) = Z_\epsilon \tan k_\epsilon\ l_\epsilon \qquad \cdots (4.5)$$

Remembering that, $Z_0/Z_\epsilon = k_\epsilon/k$, we can rewrite (4.5) as,

$$\frac{\tan k\ (D_R - D - l_\epsilon)}{k\ l_\epsilon} = \frac{\tan k_\epsilon\ l_\epsilon}{k_\epsilon\ l_\epsilon} \qquad \cdots (4.6)$$

All the quantities associated with the left hand side of eq. 4.6 are measurable, while the right hand side is in the form (tan Z)/Z, so once the measurement has been performed, the complex number, $Z = k_\epsilon\ l_\epsilon$, can be found by the solution of the transcendental equation and from it we can calculate k_ϵ. The relative permittivity ϵ_r follows directly from k_ϵ.

$$k_\epsilon = \frac{2\pi}{\lambda} \sqrt{\epsilon_r \mu_r - (\lambda/\lambda_c)^2} = \frac{2\pi}{\lambda_{g\epsilon}} \qquad \cdots (4.7)$$

Considering the fact that the tangent function is periodic in nature, there exists an infinite number of solutions for ϵ_r. Therefore, it becomes necessary either to know approximately in order to pick the right solution, or to perform a second identical experiment with a sample of

45

different length $l_{2\epsilon}$. The proper solution will then be the one common to the two sets of solution. We thus get an "intersection point", as illustrated in fig.(4.2) for a particular case. In the complex case, like the present one, equation (4.6) has been recast to achieve a more practical form (Sucher and Fox, 1963).

Procedure :

1. All the equipments were connected as shown in fig. 4.3.

2. With no sample dielectric in the short circuited line, D_R, the position of the minimum in the slotted line with respect to an arbitrarily chosen reference plane (D = 0), was found out.

3. The guide wave length, λg. was measured by measuring the distance between alternate minima in the slotted line.

4. The sample dielectric, i.e. the soil sample in this case was inserted in the short circuit to give a sample length of around $\lambda_g/4$ for best accuracy.

5. The position of the minimum in the slotted line, D with the sample in the short circuit and with respect to a reference plane (D = O) was measured.

Calculations :

For the complex dielectric constant, the calculations were as follows :
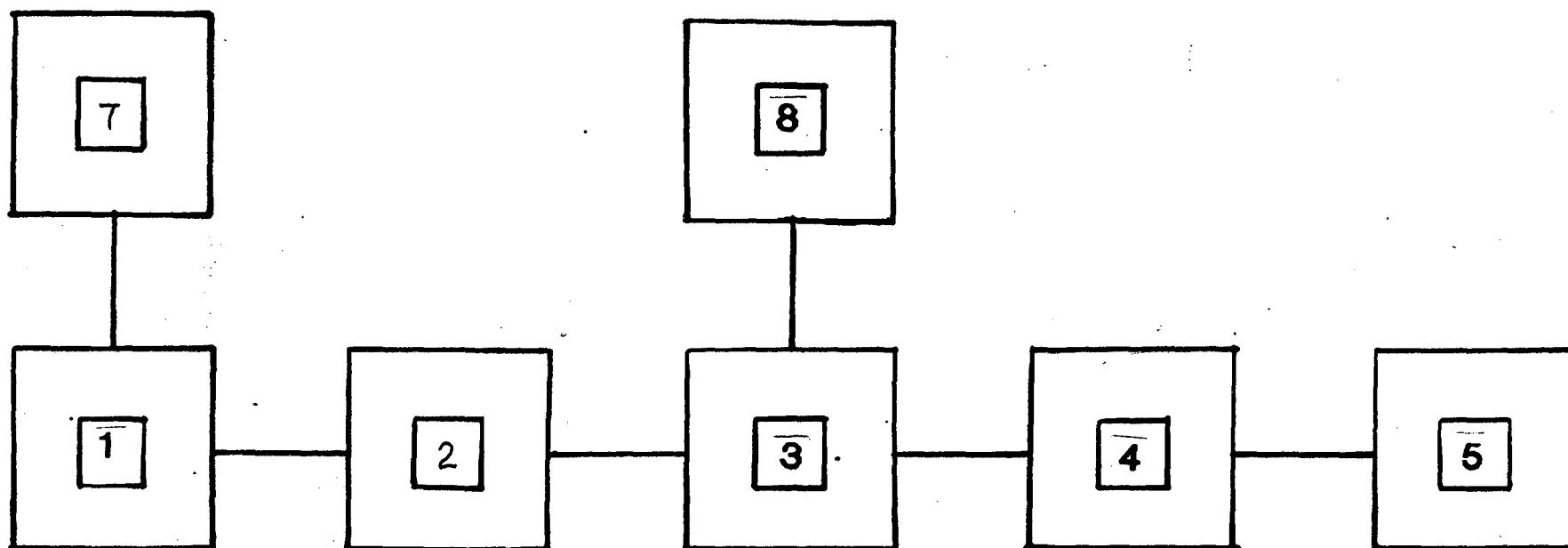
1 - GUNN OSCILLATOR

2 - ATTENUATOR

3 - SLOTTED SECTION

4 - WAVEGUIDE

5 - H-PLANE BEND

6 - DIELECTRIC CELL/
    SAMPLE-HOLDER

7 - GUNN POWER SOURCE

8 - VSWR METER

Fig 4.3: Schematic diagram of the KU band setup used for measuring ε'
by the *two point method*.

(a)   Determination of the wave number,

$$k = 2\pi / \lambda_g \qquad \cdots \ (4.8)$$

(b)   Determination of phase constant.

$$\phi = 2k \ (D - D_R - 1_\epsilon) \qquad \cdots \ (4.9)$$

(c)   Determination of reflection coefficient

$$| \Gamma | = \frac{r - 1}{r + 1} \qquad \cdots \ (4.10)$$

(d)   Determination of the complex number

$$c \underline{-\Psi} = \frac{1}{j k l_\epsilon} \cdot \frac{1 - |\Gamma| e^{j\phi}}{1 + |\Gamma| e^{j\phi}} \qquad \cdots \ (4.11)$$

In order to solve eq. (4.11), the $c - \Psi$ graph was used and the corresponding x and θ values noted directly.

These values of x and θ were then used in the calculation of Y with eq. (4.12). For the same soil sample, two closest possible values of Y for different lengths were chosen for further calculations,

$$Y = (x/kl_\epsilon)^2 \ \underline{|2(\theta - 90°)} \qquad \cdots \ (4.12)$$

The values of ϵ' and ϵ'' were then calculated from the values of x and θ as follows:

$$G = (x/kl_\epsilon)^2 \ \cos\theta' \qquad [\theta' = 2 \ (\theta - 90°)]$$

$$B = (x/kl_\epsilon)^2 \ \sin\theta'$$

$$\epsilon' = \frac{G + (\lambda_g/\lambda_c)^2}{1 + (\lambda_g/\lambda_c)^2} \qquad \cdots \ (4.13)$$

$$\epsilon'' = \frac{-B}{1 + (\lambda_g/\lambda_c)^2} \qquad \cdots \ (4.14)$$

47

The entire calculation was done with the help of a pascal program fed into a computer(see appendix II).

THE SINGLE HORN REFLECTOMETRY METHOD

Theory and Description:

The single-horn reflectometry method provides a sound technique for in situ measurement of dielectric permittivity of lossy materials through direct determination of the surface reflectivity (see Arcone et al., 1988).

In this technique, microwaves (of the desired frequency) generated from a suitable source are passed through a waveguide culminating in a standard-gain horn antenna (see fig. 4.4) onto the surface of the soil sample taken in bulk. A part of the microwaves undergo reflection at the soil surface, and the rest of it is transmitted into the medium and in due course absorbed after suffering energy loss through attenuation.

The reflectivity of the medium is measured with respect to a plane shining metal surface which provides near total reflection. The measurements, are carried out with the help of a slotted section provided in the waveguide having a movable probe connected to a VSWR meter.

The apparatus consisted of a solid state Gunn diode (adjustable to KU band frequencies) acting as the signal

source and operating around 14-15 GHz. A standard rectangular wave guide couples the Gunn oscillator to the waveguide slotted line (please refer fig 4.4) through an H-plane bend to a 6 cm by 4.4 cm aperture standard-gain horn. The slotted section is provided with a vernier scale for linear measurements of the minima shift. Besides this a VSWR meter displays the voltage standing wave ratio at the wave minima. This arrangement was also used to find out the guide wavelength λg.

The reflectometer horn aperture was placed at a suitable height (which was varied in the course of the experiment) above the soil surface. The soil was held in a perspex box.

Procedure :

1. All the equipments were connected as shown in fig 4.4.

2. With the wave guide short circuited with an empty dielectric cell, the guide wavelength ` 'λ g' was calculated by measuring the distance between alternate minima in the slotted line.

3. The horn aperture was fitted to the wave guide end and the soil sample, taken in a perspex box, placed at a particular height below the aperture.

4. The VSWR meter reading, V_s and the position of the first minima on the slotted section vernier scale, Ds

49
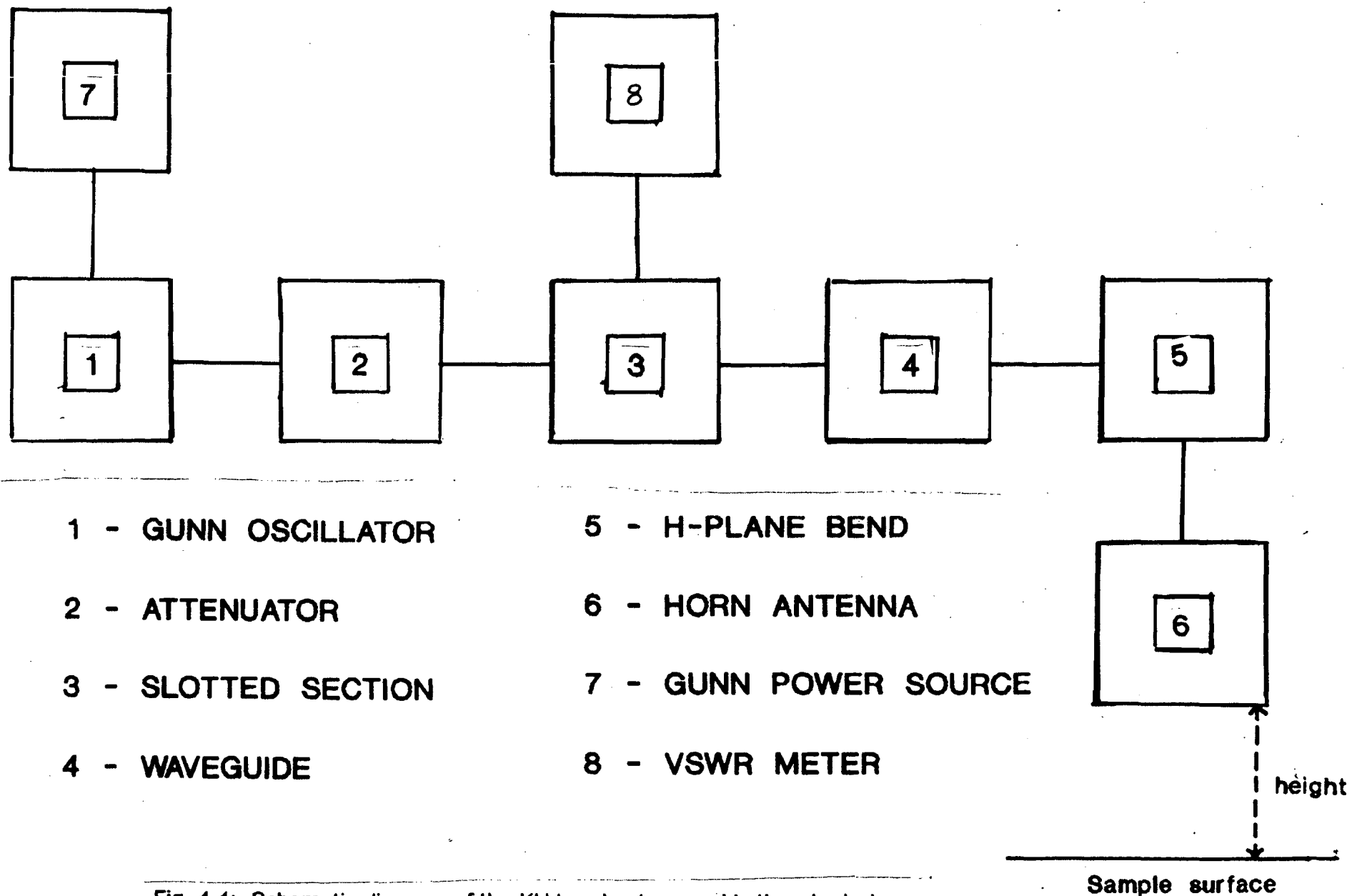
Fig. 4.4: Schematic diagram of the KU band setup used in the *single-horn reflectometry method*.

1 - GUNN OSCILLATOR

2 - ATTENUATOR

3 - SLOTTED SECTION

4 - WAVEGUIDE

5 - H-PLANE BEND

6 - HORN ANTENNA

7 - GUNN POWER SOURCE

8 - VSWR METER

are noted with the horn placed above the soil surface.

5. The soil is replaced by a shining metal surface placed exactly at the same plane below the aperture and the corresponding readings V_m and D_m noted. There was no need to adjust for the finite thickness of the metal plate as the entire box containing the soil was placed on metal plate.

6. The same procedure was repeated for different heights above the soil surface, the horn being moved a distance equal to at least 1/2 the aperture dimension each time. The experiment was further repeated with different oven dried soil samples.

Calculations :

The relative complex dielectric permittivity of the soil, $\epsilon^* = \epsilon' - j\epsilon''$ was calculated from the sample reflectivity 'ρ' measured relative to that of the metal plate using standard plane wave reflection formulation.

The magnitude of reflectivity, $|\rho|$ is given by,

$$|\rho| = \left|\frac{V_s - 1}{V_s + 1}\right| \cdot \left|\frac{V_m + 1}{V_m - 1}\right| \qquad \ldots (4.15)$$

Where 's' indicates horn above soil and 'm' indicates horn above metal plate, as mentioned earlier.

The phase ϕ of ρ was found from,

$$\phi = 4\pi\Delta x/\lambda_g \qquad \ldots (4.16)$$

Where $\Delta x = D_s \sim D_m$ (shift in the location of minima with horn above soil and horn above metal plate). λ_g is the guide wave length = 2 x distance between successive minima under short circuit conditions.

For a loss less and electrically thick dielectric (in this case soil) several wavelengths thick,

$$\epsilon = \left(\frac{1 + |\rho|}{1 - |\rho|}\right)^2 \qquad \ldots (4.17)$$

Where ρ the complex number, $\rho = \rho\, e^{j\phi}$

Although the method is best suited under field conditions the scope of the present work restricted it to laboratory conditions.

The entire calculations were carried out with the help of a fortran 77 program fed into a computer(see appendix III).

CHAPTER V

RESULTS AND DISCUSSIONS

A. Sample Collection and Analysis:

The present work was carried out with thirteen different soil samples collected from different parts of India. The physiographic divisions to which these samples belong are shown in Fig.5.1 and the soil types are illustrated in Fig. 5.2.

Three of the samples belonged to Delhi. Two of these were from the Jawaharlal Nehru University campus; one was collected from an agricultural field (JNU [1] - alluvial soil) and the other was from a relatively barren spot (JNU [2] - red sandy soil). The third sample (river bed alluvium) from Delhi belonged to a spot on the banks of the river Yamuna at Nizamuddin.

Bombay and Pune contributed two samples each to the collection. Both the samples from Bombay were dark brown alluvial soils collected from Aray Colony and the IIT Campus. The Pune samples were black cotton soils of the Deccan region collected from agricultural fields located at the Agricultural University Campus and the Botanical Garden.

52
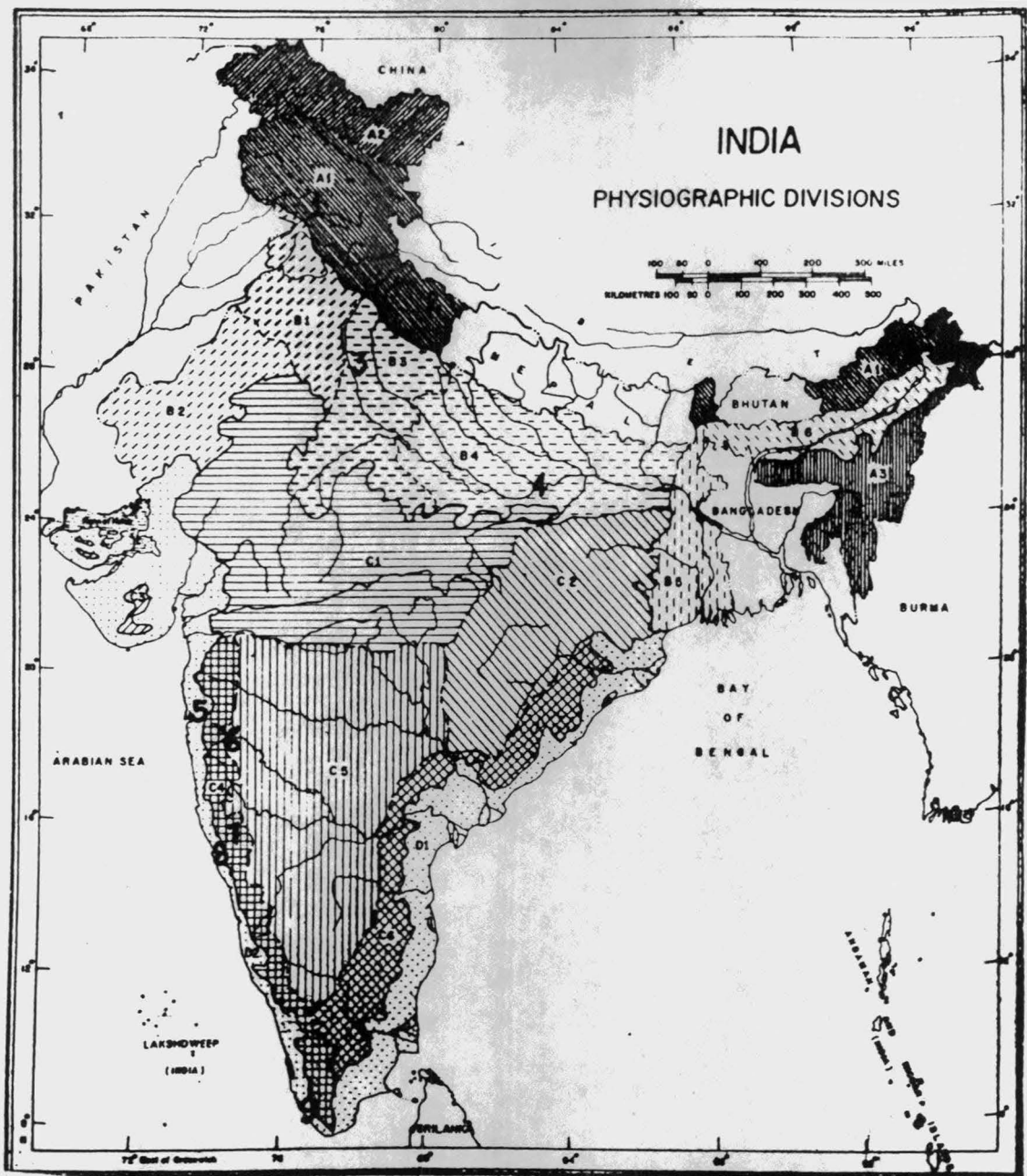
Fig.5.1: Map of India showing the physiographic divisions with the sample sites.

SAMPLE SITES

1 - KHAJJIAR
2 - GLACIER
3 - DELHI
4 - ALLAHABAD
5 - BOMBAY
6 - PUNE
7 - BELGAUM
8 - GOA
9 - KOVALAM

A1 - HIMALAYAS
A2 - TRANS HIMALAYAS
A3 - PURVANCHAL/EASTERN HILLS
B1 - PUNJAB-HARYANA PLAINS
B2 - RAJASTHAN PLAINS
B3 - UPPER GANGA PLAIN
B4 - MIDDLE GANGA PLAIN
B5 - LOWER GANGA PLAIN
B6 - BRAHMAPUTRA PLAIN

PHYSIOGRAPHIC DIVISIONS

C1 - CENTRAL PLATEAU
C2 - EASTERN PLATEAU
C3 - KATHIAWAR & KUTCH PENINSULA
C4 - SAHYADRIS(WESTERN GHATS)
C5 - DECCAN PLATEAU
C6 - EASTERN GHATS
D1 - EAST COAST
D2 - WEST COAST
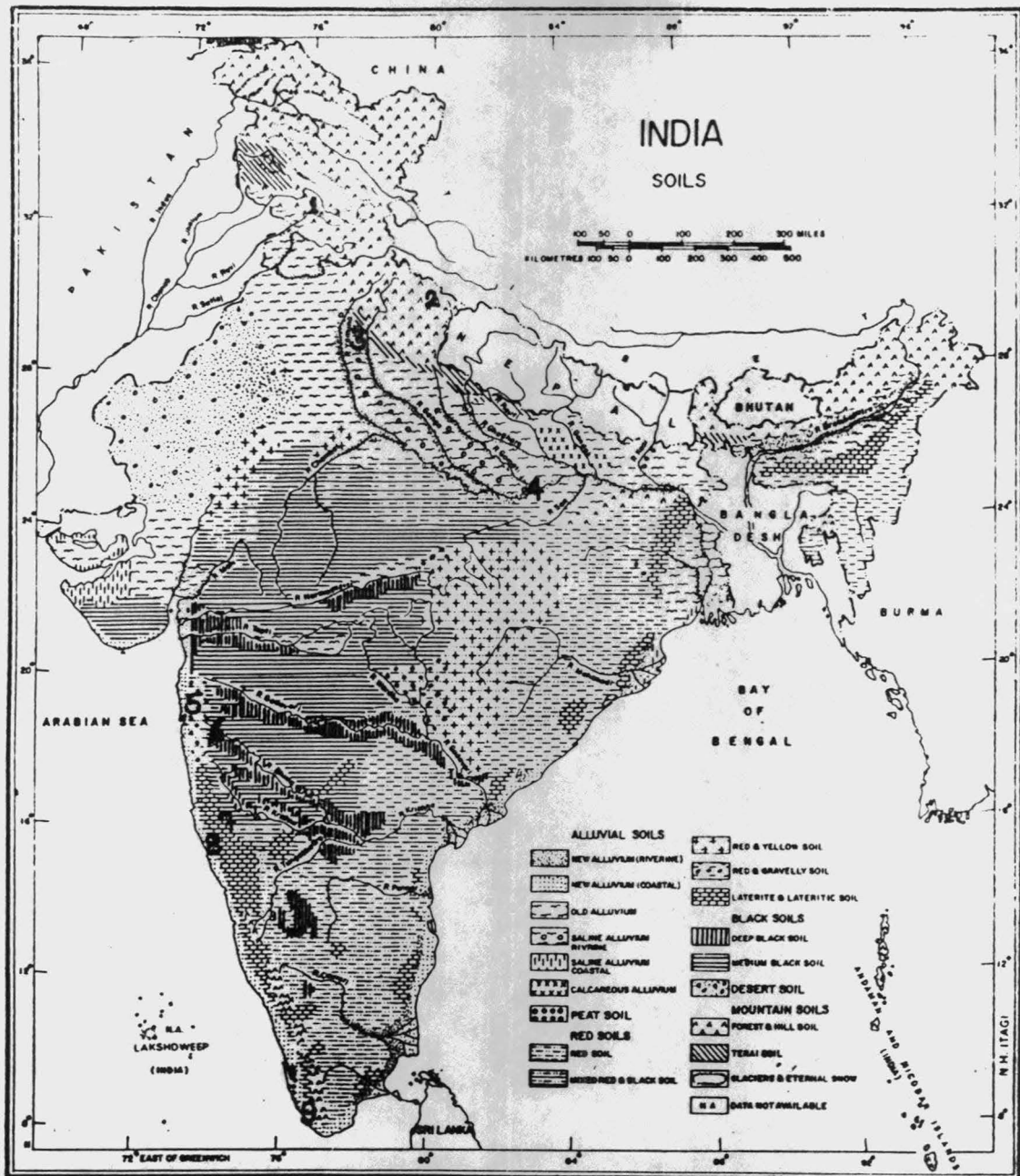
Fig.5.2: Soil map of India showing the sample sites.

SAMPLE SITES

1 - KHAJJIAR
2 - GLACIER
3 - DELHI
4 - ALLAHABAD
5 - BOMBAY
6 - PUNE
7 - BELGAUM
8 - GOA
9 - KOVALAM

The sample from Allahabad was a typical greyish alluvium of the fertile Northern Plains. On the contrary, the Belgaum sample from Karnataka was a red clay soil of the lower Deccan bordering the Western Ghat ranges.

The collection included two beach sands; one from Goa on the Konkan Coast and the other from Kovalam (near Trivandrum) on the Malabar Coast. The other two samples were collected from high up in the Himalayan mountains; one from a glacier morain (black in colour) while the other from Khajjiar in Himachal Pradesh (brown mountain soil).

The samples were first dried in an oven upto a temperature of 110°C to drive out the hygroscopic water and then passed through a 2 mm sieve to separate out the gravels and finally subjected to texture analysis by the hydrometer method (for details of the method please see Appendix I).

The results of texture analysis are shown in Table 5.1 below. The samples were also plotted on a triangular textural plot on the basis of their particle-size distribution. This is illustrated in Fig. 5.3.
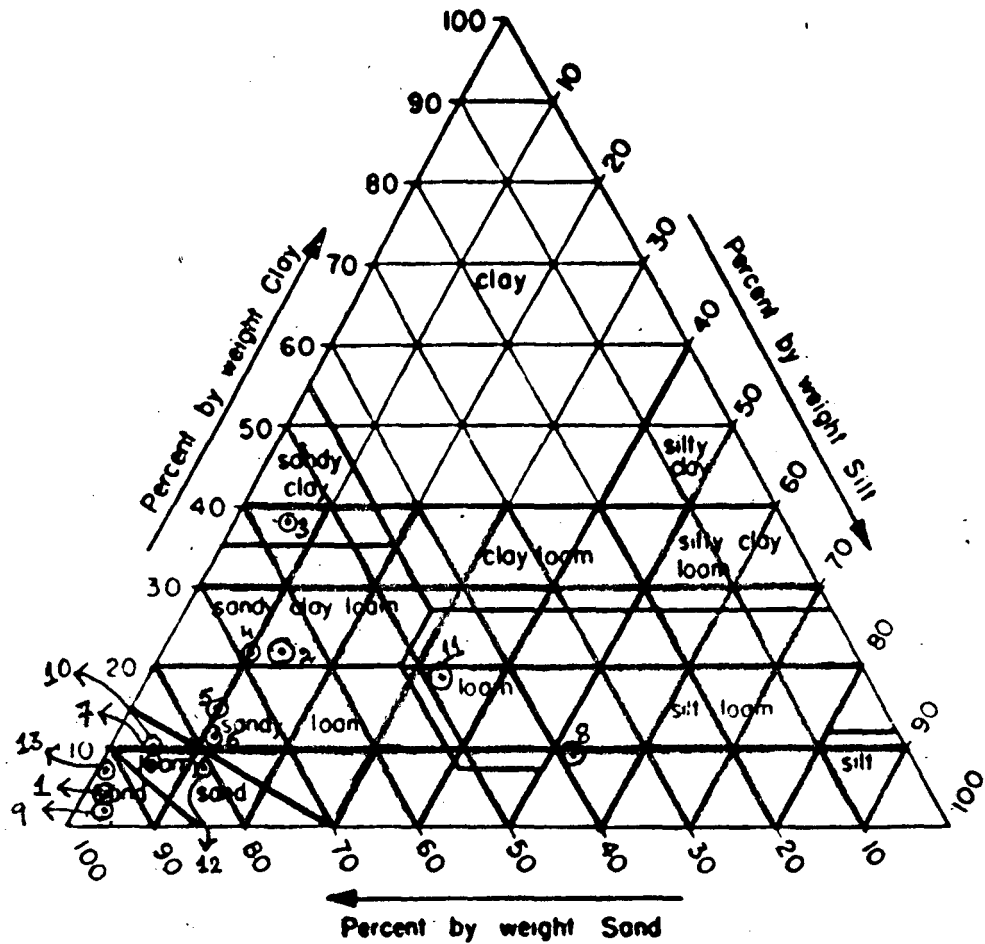
Fig.5.3: Texture triangle showing the textural classes of the samples

TABLE-5.1: RESULTS OF TEXTURE ANALYSIS

Sample No.	Place of Origin	Percentage			Textural Class
		Clay	Silt	Sand	
1.	Meraman Beach Goa	3.90	2.00	94.10	Sand
2.	Aray Colony Bombay	19.46	13.73	66.81	Sandy Clay Loam
2.	Allahabad	37.90	6.00	56.10	Sandy Clay
4.	Medical College Belgaum	20.50	10.00	69.50	Sandy Clay Loam
5.	Agricultural Univ. Pune	14.50	10.00	75.50	Sandy Loam
6.	IIT, Bombay	12.50	9.00	78.50	Sandy Loam
7.	Botanical Garden Pune	8.90	5.20	85.90	Loamy Sand
8.	JNU Campus (1) New Delhi	9.90	52.00	38.10	Silt Loam
9.	Kovalam Beach Kerala	3.80	2.10	94.10	Sand
10	JNU Campus (II) New Delhi	9.90	5.90	84.20	Loamy Sand
11	Khajjiar, Dist. Chamba; Himachal	19.10	32.90	48.00	Loam
12	Nizamuddin, New Delhi	9.10	10.60	80.30	Loamy Sand
13	Glacier	7.21	0.74	92.05	Sand

B. Results and Analysis of Dielectric Parameter Measurements:

I. Sample Treatment:

The samples were first dried in an oven for 24 hrs at a temperature of 110°C. This was to ensure the complete evaporation of hygroscopic water which remains in the soil till 105°C. The dried samples were cooled in a dessicator and subjected to light grinding to ensure the absence of any soil clots and then sieved through a 2 mm sieve in order to separate out the gravel (particles with d>2mm).

The bulk density (ρ_b) of the samples were determined by measuring the weights (m_b) of known volumes (v_b) of the samples. Then bulk density is given by:

$$\rho_b = m_b/v_b \qquad \qquad \dots (5.1)$$

The measurements were first carried out on dry samples. Then, a known volume of water was added to a known weight (W_d) of each dry sample. The weight of the wet samples W_w was recorded before the start of the experiment and after the experiment the sample was again dried, cooled and its weight recorded to give the dry weight (W_w).

The gravimetric moisture content (m_g) was calculated by the formula:

$$m_g = \frac{\text{Weight of Wet Sample} - \text{Wet of Dry Sample}}{\text{Weight of Dry Sample}} \qquad \dots (5.2a)$$

$$\text{i.e. } m_g = \frac{(W_w - W_d)}{(W_d)} \qquad \dots (5.2b)$$

The volumetric moisture content (m_v) was then calculated by:

$$m_v = m_g \times \rho_b \qquad \dots (5.3)$$

After each water addition, the sample was allowed to stand for 24 hours to facilitate internal drainage and subsequent homogeneous mixing of soil and water.

II. The Two Point Method:

The values of ϵ'_{soil} and ϵ''_{soil} for each sample obtained by the two-point method were plotted against the volumetric moisture content (m_v) as shown in Figs. 5.4, 5.5 and 5.6. The plots were obtained with the help of a curve fitting technique. The general guiding equation for all the curves of Figs. 5.4, 5.5 and 5.6 is of the form y = a*exp(x/b) with the coefficients a and b assuming closely placed but differing values in each case. The scattering of the data points about the curves was found to be not more than 5% predicting a homogeneity in the results obtained. The values of the coefficients "a" and "b" are shown in Table 5.2 below.
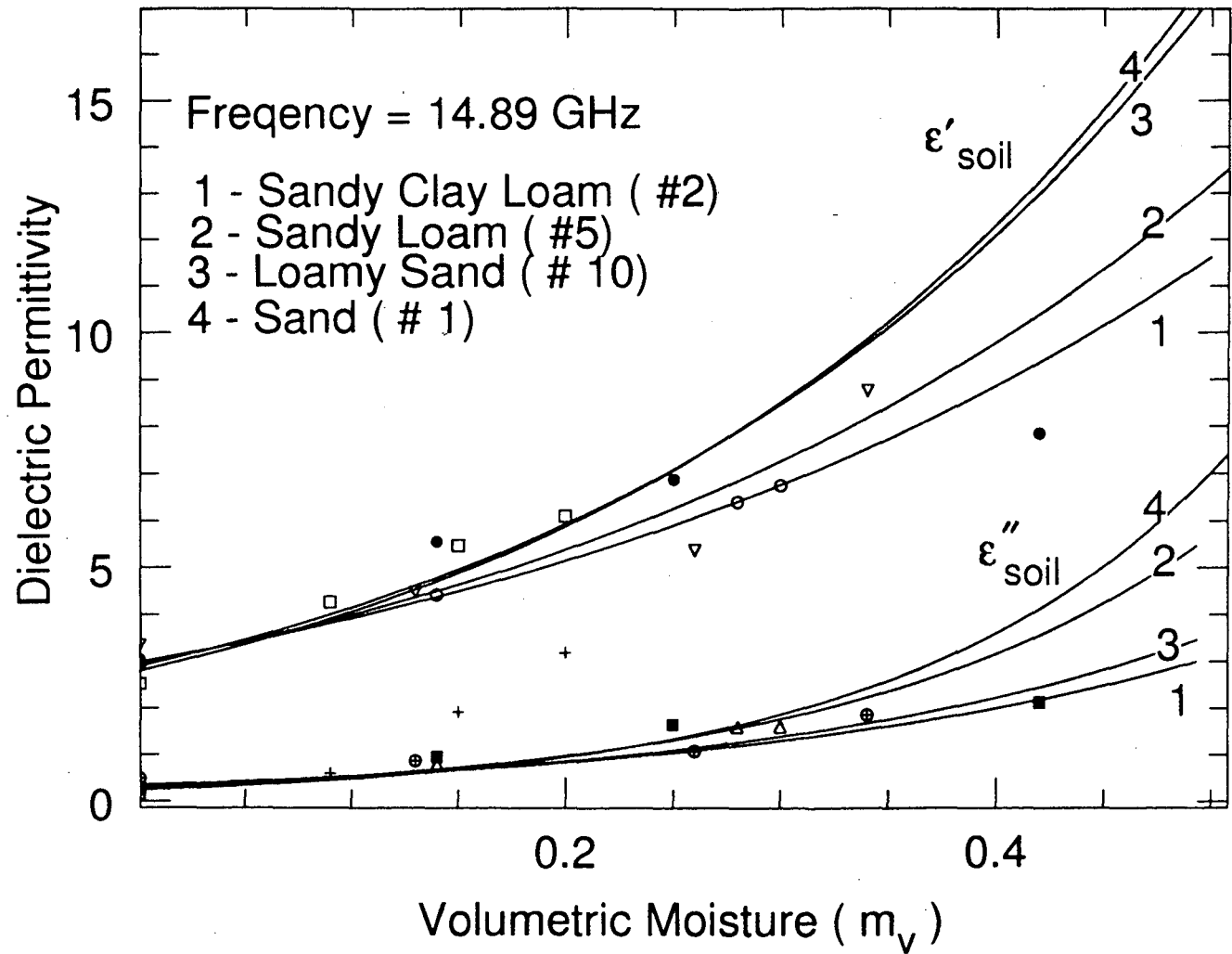
Fig.5.4: Dependence of dielectric permittivity on soil moisture and texture for four samples.
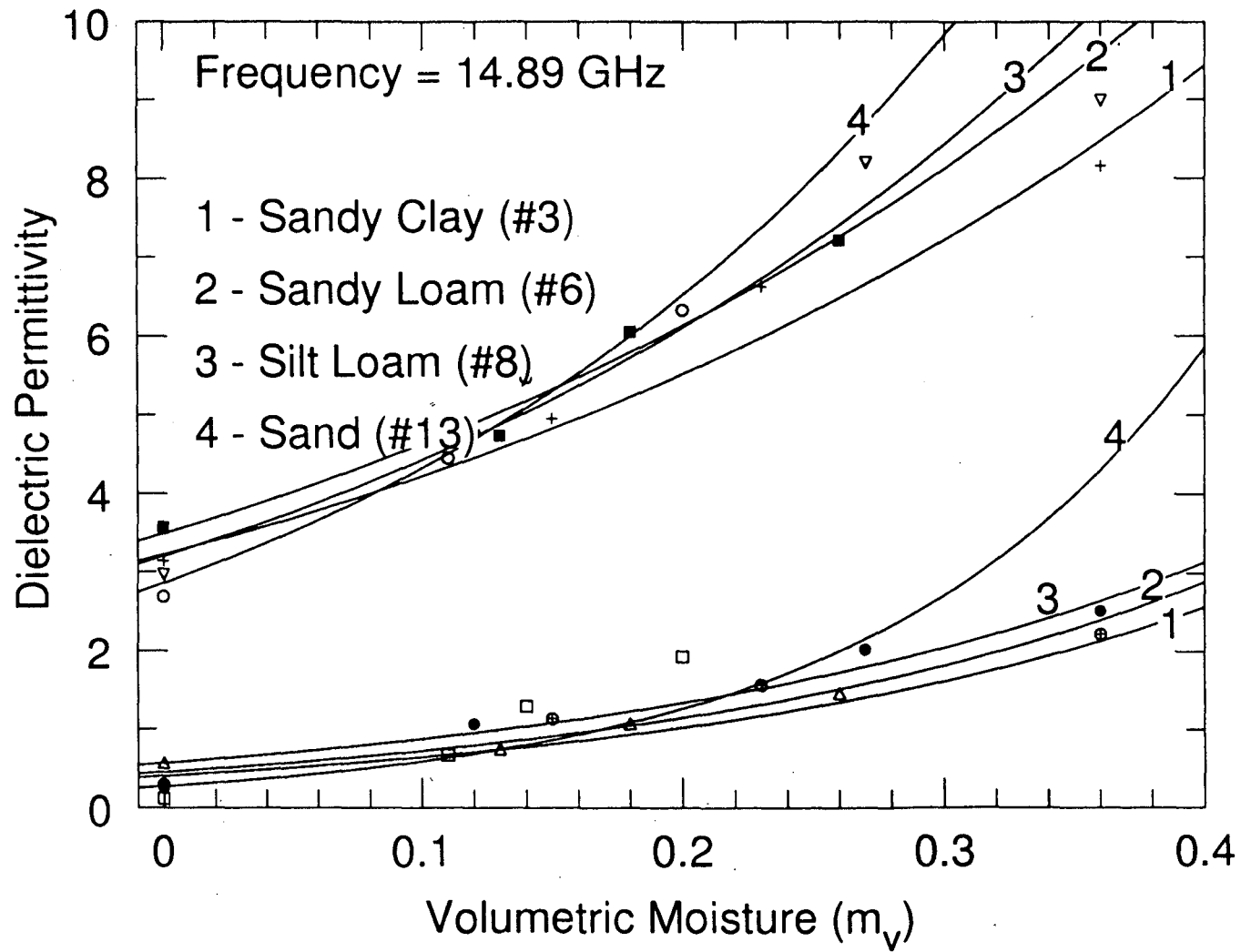
Fig.5.5: Dependence of dielectric permittivity on soil moisture and texture for four samples.
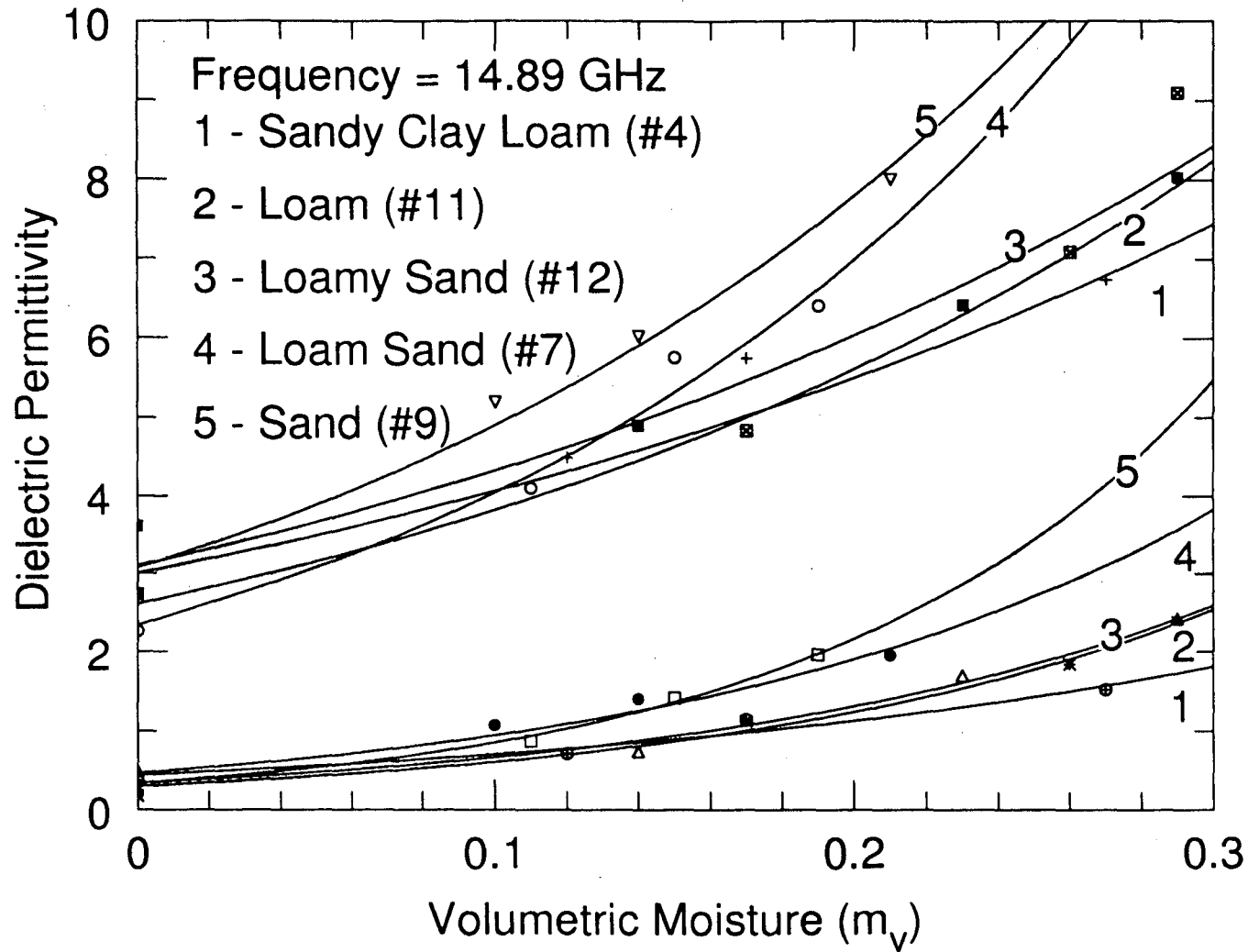
Fig.5.6: Dependence of dielectric permittivity on soil moisture and texture for five samples.

TABLE 5.2: Curve Fitting Data

Fig. No.	Curve No.	ϵ'(soil) a	ϵ'(soil) b	ϵ''(soil) a	ϵ''(soil) b
5.4	1	2.98	0.36	0.35	0.17
5.4	2	2.95	0.33	0.33	0.21
5.4	3	2.90	0.28	0.30	0.17
5.4	4	2.80	0.27	0.25	0.15
5.5	1	3.22	0.37	0.56	0.22
5.5	2	3.49	0.36	0.45	0.22
5.5	3	3.20	0.31	0.56	0.23
5.5	4	2.85	0.24	0.27	0.13
5.6	1	2.33	0.18	0.34	0.11
5.6	2	3.07	0.21	0.33	0.20
5.6	3	3.10	0.30	0.34	0.14
5.6	4	3.00	0.33	0.43	0.21
5.6	5	2.60	0.26	0.30	0.14

A study of the table reveals that the value of the coefficient "a" which decides the $m_v = 0$ intercept of the curve is very closely spaced for any group of curves both for ϵ'(soil) and ϵ''(soil). However, the value of the

57

coefficient "b" which determines the slope of the curve seems to vary a lot with the soil texture. This implies that under dry conditions, soil texture has little effect on the value of dielectric permittivity but this behaviour changes with increase in the water content.

The general behaviour of ϵ'_{soil} as a function of moisture content and soil texture can be summarised as follows:

i) ϵ'_{soil} was seen to increase gradually with increasing moisture content till a certain transition point W_t for all the samples. Beyond the transition point the increase is much rapid for all the samples. The transition point W_t was observed to be dependent on the clay content of the sample. As has already been pointed out in Chapter III, and also in the works of previous investigators (Hallikainen et al., 1985; Geiger et al., 1972; Hoekstra et al., 1974; Wang et al., 1978; Alex and Behari, 1996 to mention a few). This is due to the large specific surface area of clay particles in comparison to the other basic components of soil; silt and sand. The large specific surface area of clay particles enable them to retain more water in the form of bound water. Now, the dielectric permittivity of bound water is quite lower than that of the bulk free water. When water is added to a clayey soil a greater portion of it is adsorbed as

bound water relative to silt and sand. This phenomenon results in wet clayey soils having a lower net dielectric constant than wet silty and sandy soils at the same moisture level resulting in a higher transition point for the former.

ii)The value of ϵ'_{soil} was noticed to be approximately proportional to the sand content. This is due to the `bound water' factor and the "salinity" factor. Sand having a lower specific surface area has more of `free water' than bound water at a given moisture content resulting in a higher dielectric constant. Secondly, the low specific surface area results in a lower cation exchange capacity for sand as compared to clay. This means that sandy soils are not as open to various physico-chemical processes as clayey soils resulting in a lower salinity of the soil water mixture in case of sand. The presence of mineral salts de crease the dielectric constant of water and conversely as in this case, their absence keeps it high.

The behaviour of the dielectric loss factor ϵ''_{soil} can also be summarised along similar lines but requires an understanding of the phenomenon of dielectric relaxation which absorbs energy in a dielectric medium. When a dielectric medium is subjected to an alternating field, as in the present case, it undergoes a change in the orientation of its dipole moments with the sinusoidally

varying field leading to the phenomenon of dielectric relaxation. At low frequencies, the varying dipole field may be in phase with the applied sinusoidal field. But in case of high frequencies like that used in the present work, a phase lag will creep in. As a result of this phase lag, the dipoles, in order to overcome the same, tend to absorb more and more energy from the applied field leading to an increase in the dielectric loss factor.

It was observed that, like the dielectric constant ϵ', the loss factor ϵ'' also increased with increase in moisture content, gradually at first and more steeply beyond a transition point. The dielectric loss was proportional to the sand content and inversely proportional to the clay content. Clayey soils in general had a lower loss factor at a given moisture level and were characterized by a higher transition point.

This phenomenon is again explained by the larger specific surface area of clay particles. By virtue of their higher cation exchange capacity, a greater number of physical and chemical processes are facilitated causing a large concentration of salts in the soil water solution. An increase in the salt concentration increases the ionic concentration resulting in greater ionic conductivity. The end effect is a lower loss factor. But as the water content

is increased, the specific ionic concentration falls leading to an increase in the loss factor finally reaching a transition point beyond which the increase is very sharp.

III. Field Capacity, Wilting Point and Transition Point of the Samples:

Soil parameters like *field capacity* (FC), *wilting point* (W_p) and *transition point* (W_t) were calculated using the Wang and Schmugge model (1980). By this model:

$$FC = 25.1 - 0.21 \text{ Sand } (\%) + 0.22 \text{ clay } (\%)$$

$$W_p = 0.06774 - 0.00064 \text{ sand } (\%) + 0.00478 \text{ clay } (\%)$$

$$W_t = 0.49 \, W_p + 0.165$$

The results of the calculation are shown in Table 5.3 below:

TABLE 5.3: SOIL PARAMETERS

Sample No.	Field Capacity (FC)	Wilting Point (W_p)	Transition Point (W_t)
01.	6.20	0.03	0.18
02.	15.35	0.12	0.22
03.	21.66	0.21	0.27
04.	15.02	0.12	0.22
05.	12.44	0.09	0.21
06.	11.37	0.08	0.20
07.	9.02	0.06	0.19
08.	19.28	0.09	0.21
09.	6.18	0.03	0.18
10.	9.60	0.06	0.20
11.	19.22	0.13	0.23
12.	10.24	0.06	0.19
13.	7.36	0.04	0.19

A comparison of Tables 5.1 and 5.3 immediately reveals that both the parameters FC and W_t are dependent on the clay fraction present in soil and increase with the same. Once again, this is attributed to the large specific surface area of clay. The capacity of clay to hold water in the bound molecular form gives it a greater field capacity and transition point and thus wilting point also.

Such parameters are useful for the knowledge of agricultural and soil scientists. A high field capacity or transition point derived directly from dielectric parameter measurements means presence of a greater content of clay which will facilitate physicochemical processes on the soil surface leading to release of essential macronutrients for the plants. Moreover, a high wilting point indicates that plants can smoothly tide over the dry waterless season.

IV. Emissivity Calculations:

The value of emissivity "e" was calculated by using the formula,

$$e = 1 - \left| \frac{1 - \sqrt{\epsilon'}}{1 + \sqrt{\epsilon'}} \right|^2$$

The values of emissivity so calculated for samples of

different texture were plotted against volumetric moisture content. The result is shown in Fig. 5.7. The results agree quite well with the research of previous investigators like Dobson et al.,(1984).

A study of the plot reveals, two notable features, viz. (i) the microwave emissivity from bare soil surfaces decrease with increase in moisture content of the surface, and (ii) microwave emissivity is almost independent of the soil texture for dry soils.

The first property of microwave emissivity, i.e. its decrease with increase in water content makes it the most sought after parameter in the study of soil moisture profile through microwave remote sensing. Microwave emissivity can thus directly be linked to the moisture profile of the soil of any region.

As far as the second feature is concerned, a number of investigators (Schmugge, 1980; Rouse Jr., 1983; Dobson et al., 1984) have attempted to overcome the texture effect by plotting the microwave emissivity against a new unit, *percentage of field capacity* ($M_{fc} = M_g/FC$) in place of the usual gravimetric moisture (m_g) or volumetric moisture (m_v) units. It was observed by them that in the case of per cent field capacity the texture effect was overcompensated unlike the plots against m_g and m_v. In Fig 5.8, the
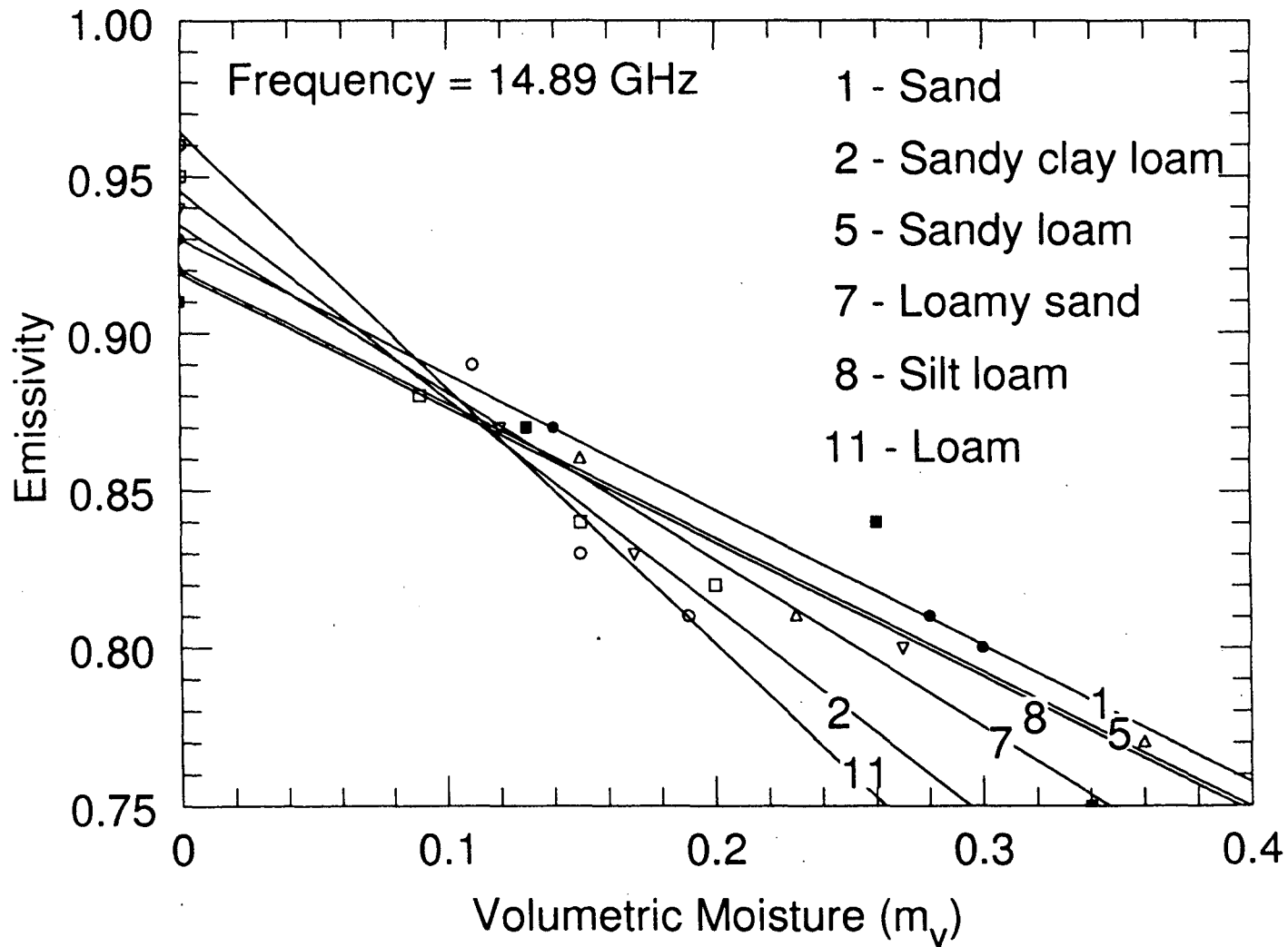
Fig.5.7: Variation of microwave emissivity with volumetric moisture. (refer table 5.1 for soil compositions).
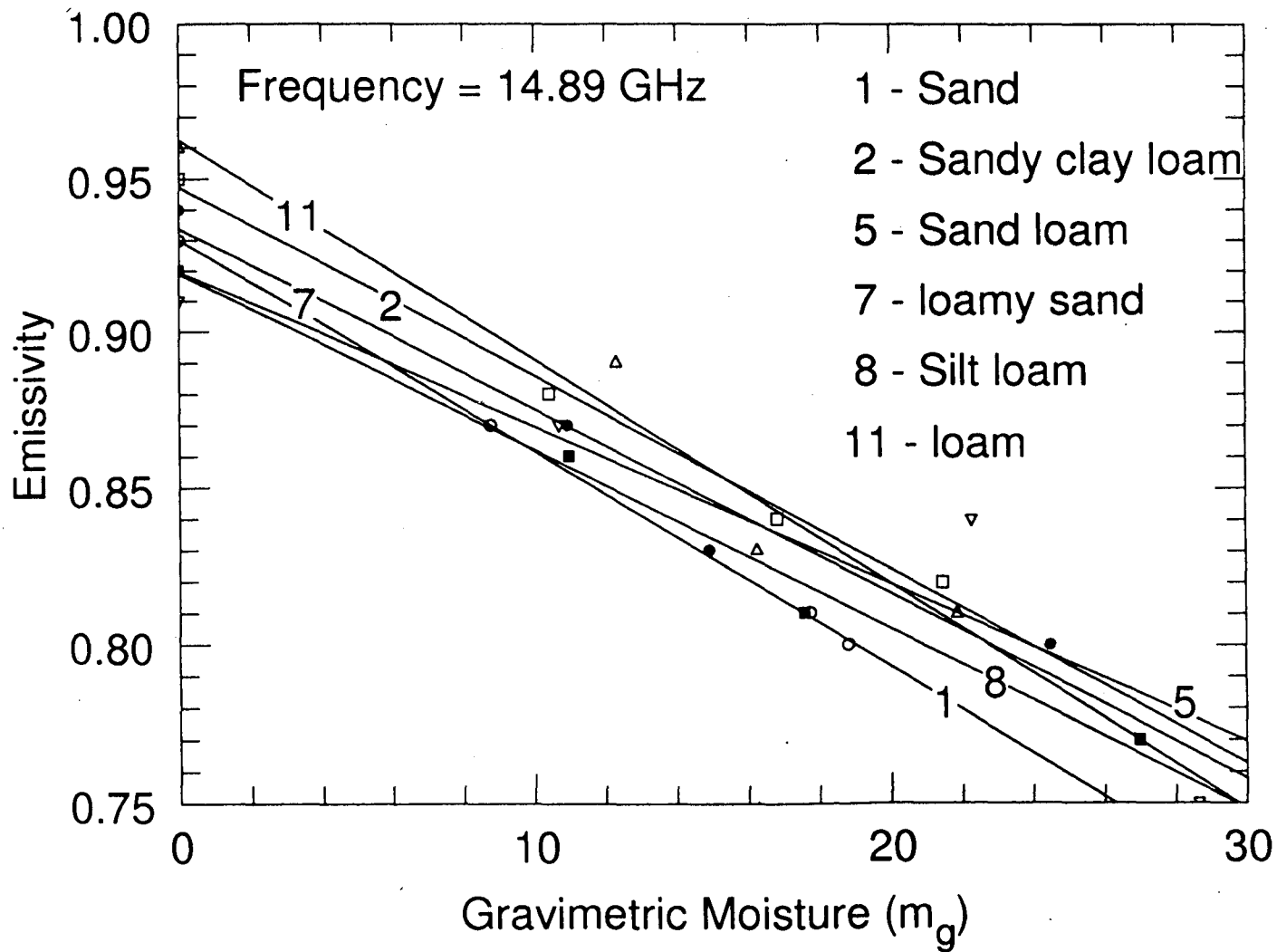
Fig.5.8: Variation of microwave emissivity
with gravimetric moisture. (refer
table 5.1 for soil compositions).

emissivity has been plotted against the gravimetric moisture content (M_g). In case of Fig. 5.8 also, the straight best fits appear to diverge more at higher water contents than at dry moisture levels behaving more or less as in the plot of Fig. 5.7. The intercepts at $M_g = 0$ and $M_v = 0$ are a bit scattered. If we take into consideration minor discrepancies due to instrumental error then we may conclude that for all practical purposes microwave emissivity is independent of soil texture for bare surfaces under dry conditions. Under normal wet conditions i.e., water content $\leq$ 10% this situation does not seem to change. Both the plots , however point out that at high (>10%) water contents soil texture comes into picture and starts affecting the variation of microwave emissivity with soil moisture level albeit, marginally.

V. <u>The Single-horn Reflectometry Method</u>:

Dielectric permittivity and Reflectivity of three dry soil samples were measured by the single-horn reflectometry method. The results are shown in Figs. 5.9 and 5.10.

In Fig. 5.9 the value of reflectivity is plotted as a function of the height of horn antenna above the sample surface. At heights above 11 cm, the curve smoothens out indicating a stable value of reflectivity. The nature of the plot is similar to that obtained by Arcone et al., (1988),
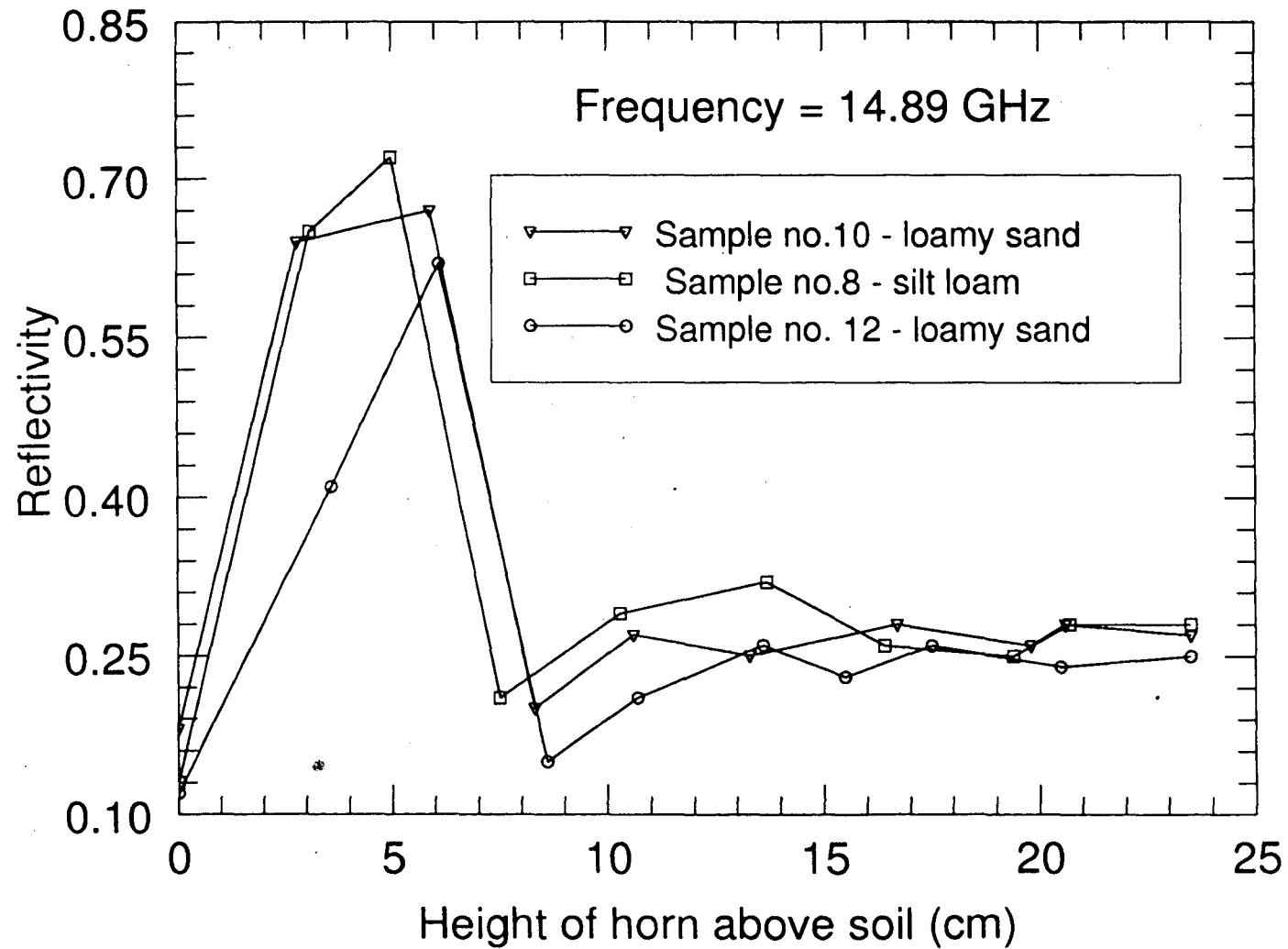
Fig.5.9: Variation of surface reflectivity
with height of horn above sample
plane (refer table 5.1 for soil
compositions).
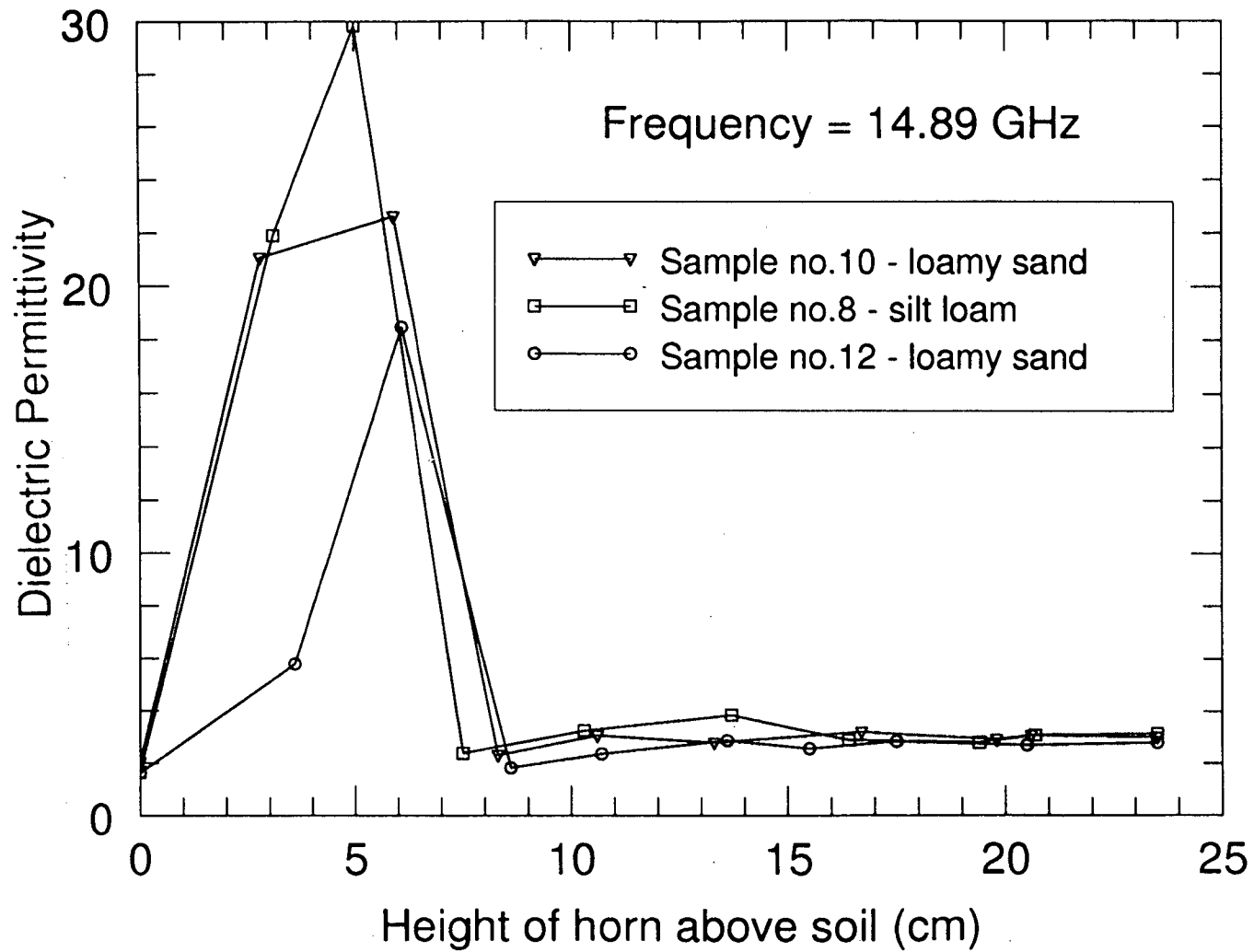
Fig.5.10: Variation of dielectric permittivi-
ty with height of horn above sample
plane (refer table 5.1 for soil
compositions).

reflectivity, it was expected that the permittivity will attain a stable value at heights above 11 cm. This prediction is confirmed in the plot of Fig. 5.10.

In order to obtain greater accuracy the value of dielectric permittivity was calculated for different heights ranging between 11-24 cm. The average of these values was taken as the final value of dielectric permittivity obtained by this method. The final values so obtained agree quite well with the values obtained by the two point method. This is shown in Table 5.4 below.

TABLE 5.4; DIELECTRIC PERMITTIVITY BY THE REFLECTOMETRY METHOD AND COMPARISON WITH TWO POINT METHOD

Sample No.	Height above sample (cm)	Value of ϵ'	Value of ϵ''	Average ϵ'	Average ϵ''	Value by Two-Point Method ϵ'	ϵ''
12.	13.6	2.85	0.30				
	15.5	2.55	0.22				
	17.5	2.83	0.08	2.74	0.16	2.74	0.20
	20.5	2.69	0.09				
	23.5	2.79	0.11				
8.	13.7	3.82	0.29				
	16.4	2.88	0.18				
	19.4	2.80	0.26	3.14	0.25	3.14	0.29
	20.7	3.08	0.20				
	23.5	3.14	0.32				
10.	13.3	2.77	0.13				
	16.7	3.19	0.20				
	19.8	2.92	0.28	2.99	0.23	3.04	0.29
	20.6	3.07	0.32				
	23.5	3.01	0.24				

(Please refer to Table 5.1 for the texture of the samples)

The close overlapping of the plots in Fig. 5.9 indicates that there is very little dependence of reflectivity on soil texture. In fact, amongst the three parameters soil dielectric permittivity, soil microwave emissivity and soil microwave reflectivity, the latter appears to be the least dependent on texture under dry soil conditions.

C. Concluding Remarks:

Different investigators over the past two decades (Dobson, Hallikainen et al., 1985; Hoekstra and Delaney, 1974; Lundien, 1971; Schmugge, 1980; Wang and Schmugge, 1980) have concluded that the dielectric constant of soil and water is not an weighted average like that of other mixtures involving water.

The results obtained in the present study also points out the dependence of the dielectric constant and the dielectric loss factor upon soil texture. The clay fraction which holds the bound water is the governing component of soil which determines its moisture content, water holding capacity and dielectric permittivity. Changes in the clay fraction affects strongly the moisture content which in turn affects the dielectric constant. This property has been utilised in several experiments involving microwave remote sensing.

sensing.

Microwave emissivity depends on a number of parameters like surface roughness, vegetation cover, etc. The study of these effects are still under progress and there are a lot of unexplained behaviours which have confused the pioneers in this field. The effect of vegetation cover on dielectric constant at different soil moisture profiles would prove to be an interesting extension of the present work.

Since, the reflectometry method involves samples taken in a bulk quantity when compared to the two point method (which involves a very small quantity of the sample), it is best suited for field observations. But this kind of laboratory measurements are necessary for standardisation of the instrument before conducting field studies. The present observations have been carried out at normal incidence over soil surface. The main disadvantage of this method is that the measurements are greatly affected by surface roughness and the angle of incidence. An extension of this work would then be to carry on the study at different moisture levels for different grazing angles and surface roughness.

The close agreement of the results obtained by these two methods point out the accuracy of the measured values. The dielectric loss factor depends on the mode of packing of the soil. The fundamental difference between the two methods

is that inthe two-point method, the soil sample is confined to a short-circuited waveguide while in the reflectometry method it is taken in an open box in a more radiative environment. The mode of packing being different in the two cases might have resulted in a slight disagreement in the values of the loss factor in the two cases. Moreover, in the reflectometry method the sample was not taken in an anechoic chamber in order to closely simulate it to field conditions. As a result, reflections from surrounding surfaces might have interfered with the reflected waves from the soil surface leading to slightly diferent loss factor values.

It is hoped that this work would prove to be an useful data bank on Indian soils and be of utmost utility to those who wish to carry out further field observations.

BIBLIOGRAPHY

Books and other Publications

Allen, S.E.(1974), Chemical Analysis of Ecological Materials". Blackwell Scientific Publication, pp.23-24.

Baver, L.D., Gardner, W.H. and Gardner W.R. (1977), Soil Physics. New York Wiley, 1977.

Bear, F.E. (1955). Chemistry of Soils. Reinhold New York.

Bottcher C.J.F. Theory of Electric Polarization. Elsevier Publ.Co., Amsterdam, 1952.

Bottcher, C.J.F. and P. Bordwijk. Theory of Electric Poliarization. Vol.2, Elsevier Publ. Co. Amsterdam 1978.

Brady C. Nyle. The Nature and Properties of Soils. Macmillan Publishing Co. INC, USA, 1984.

Davis, J.L., G.C. Topp and A.D. Annan. Electromagnetic Detection of Soil Water Content. Progress Report II. Workshop Proc. Remote Sensing of Soil Moisture and Groundwater, Royal York Hotel, Toronto, Canada, 1976.

Geiger, F.E. and D. Williams. Dielectric Constants of Soils at Microwave Frequencies. NASA TMS-65987, Washington, D.C., 1972.

Grim, R.E. Organization of water on clay mineral surfaces and its implications for the properties of clay water systems. Water and its conduction in soils. Highway Res. Board. Spec. Rep 40. Nat. Acad. Sci. - Nat Res. Council Publ. 629, pp.17-23, 1958.

Hill N.E., W.E. Vaughan, A.H. Price and M.H. Davis. Dielectric properties and molecular behaviour. Van Nostrand, Reinhold, London, 1969.

Hillel Daniel. <u>Soil and Water, Principles and Processes</u>. Academic Press, New York and London, 1973.

Jedlicka, R.P., <u>Saline Soil Dielectric Measurements</u>, Master's Thesis, New Mexico State University, Las Cruces, NM, 1978.

Lundien, J.R. <u>Terrain Analysis by Electromagnetic Means</u>, Tech. Rep. 3-727, U.S. Army Engineer Waterways Experiment Station, Vicjsburg, MS. 1971.

Marshall, T.J. and Holmes, J.W. (1988), <u>Soil Physics</u>, Cambridge University Press, Cambridge.

Montgomery, C.G. (ed.) <u>Dielectric Materials and Application</u>, The Technical Press, MIT and John Wiley & Sons, New York, 1961.

MusiI, J. & Zacek, F. (ed.). <u>Microwave Measurements of Complex Permittivity by Free-Space Method and their Application</u>, Elsvier Publishers, Amsterdam-Oxford-New York-Tokyo, 1986.

Newton, R.E. W.R. McClellan. <u>Permittivity Measurements of Soils at L-Band</u>, Tech. Rep. RSC-58, Texas A&M, University College Station, TX. 1975.

Poe, G. A. Stagryn. and A.T. Edgerton, <u>Determination of Soil Moisture Content Using Microwave Radiometry</u> Final Tech. Rep. 1684-1. Aerojet General Corp. EL. Monte. CA. 1971.

Poe. G. <u>Remote Sensing of the Near-Surface Moisture Profile of Specular Soils with Multi-Frequency Microwave Radiometry</u>. Proc. SPIE Seminar on Remote Sensing of Earth Resources and the Environment. Palo Alto. CA. pp. 135-145, 1971.

Sharma, T.C. and Cautinho. O. (1988). <u>Economic and Commercial Geography of India</u>. Jugnu Offset. Delhi.

Smyth, C.P. <u>Dielectric Behaviour and Structure</u>, McGraw Hill Book Co. Inc., New York, Toronto, London. 1955.

Steila, D. 1976. The Geography of Soils, formation, distribution and management. Prentice Hall Inc., New Jersey.

Sucher, M. and J. Fox Handbook of Microwave Measurements. Vol.II Polytechnic Press of the Polytechnic Institue of Brooklyn. 1963.

Von Hippel, A.R., Dielectric Materials and Applications. The Tech. Press of M.I.T. and John Wiley and Sons Inc., New York, 1961.

Papers

Alex, Z.C., Behari, J. and Zaidi, Z.H. (1994). "Biological tissue characterization at microwave frequencies: A Review". Technical Review, IETE, Vol.II, No.1.

Alex, Z.C. and Behari, J (1996). "Complex dielectric permitivity of soil as function of frequency, moisture and texture". Indian J. Pure and Applied Physics. 34: 319-323.

Arcone, S.A. and Larson, R.W. (1988). "Single horn reflectometry for in situ dielectric measurements at microwave frequencies". IEEE Trans. Geosci. Remote Sensing, 26: 89-92.

Aruna, R. and Behari, J. (1981). "Dielectric loss in biogenic steroid at microwave frequencies". IEEE. Trans. on Micro Theo. and Tech. Vol.29, no.11 pp. 1209-1213.

Bayser, A. and Kuerter, J.Z. (1992). "Dielectric property measurements of materials using the cavity technique". IEEE Trans. Micro. Theo. Tech. MTT. 40: 2108-2110.

Behari, J., Haresh Kumar and Aruna, R. (1982). "Effect of ultraviolet light on the dielectric behaviour of bone at microwave frequencies". Annals of Biomedical Engineering 10: 139-144.

Bethe, H.A. and Schwinger (1943). "Perturbation Theory of Resonant Cavities". J. NRDC Report, Vol.D, pp.4-117.

Birenbaum, L. and Grosof, G.N. "Effect of Microwaves, on the eye". <u>IEEE Trans Bio Med. Engg</u>. BME-26, 7-14.

Boifot, A.M. "Broad Band Method for Measuring Dielectic Constant of Liquids using an automatic network analyzer". <u>IEEE proc</u>.136, pt.H. 492-498.

Buckmaster, H.A., Hansen, C.H. and Zaghloul, H. 1985). "Complex Permittivity Insturmentation for High Loss Liquids at microwave frequencies". <u>IEEE Trans. Microwave Theory Tech</u>. MTT-33 : 822-824.

Burke, K.H. and Schmugge, T.J. (1982). "Effects of varying soil moisture contents and vegetation canopies on microwave emissions". <u>IEEE Trans. Geo Sci. Remote Sensing</u>, GE-20:268-274.

Campbell, M.J. and J. Ulrichs, "Electrical Properties of rocks and their significance for lunar radar observations". <u>J. Geophysics. Res</u>., Vol.74, pp.5867-5881, 1969.

Dobson, M.C., Kouyate, F and Ulaby, F.T. 1984). "A reexamination of soil textural effects on microwave emission and backscattering. <u>IEEE Trans. Geo Sci</u>. Remote Sensing, GE-22: 530-536.

Dobson, M.C., Ulaby, F.T., Hallikainen, M.T. and El-Rayes, M.A. (1985). "Microwave dielectric behaviour of wet soil - Part II : Dialectic Mixing Models". <u>IEEE Trans. Geo Sci. Remote Sensing</u>, GE - 23 : 35-46.

Evans, S. "Dielectric properties of Ice and Snow - A Review". <u>J. Glaciol</u>, 5, pp.773-792, 1965.

Ferrazzoli P., Paloscia, S., Pampaloni, P., Schiavon G. Solimini, D. and Coppo, P. (1992). "Sensitivity of Microwave Measurement to vegetation bio-mass and soil moisture content - A case study". <u>IEEE. Trans. Geo Sci. Remote Sensing</u>. 30: 750-756.

72

Fujita, S., Shiraishi, M. and Mae, S. (1992). "Measurement on the dielectric properties of acid-doped ice" at 9.7. GHz. IEEE Trans. Geo Sci. Remote Sensing 30:799-803.

Ganchev, S.I., Bakhtiari, S. and Zoughi, R. 1992). "A novel numerical technique for dielectric measurement of generally lossy dielectrics". IEEE Trans Instru. Measurements, 41 : 361-365.

Hallikainen, M.T., Ulaby, F.T., Dobson, M.C., El-Rayes, M.A. and Wu, L.K. (1985). "Microwave dielectric behaviour of wet soil - Part I. Empirical Models and Experimental Observations". IEEE Trans. Geo Sci. Remote Sensing, GE-23 : 25-34.

Hill, R.M. "Nature", 275, pp.96, 1978.

Hipp, J.E. "Soil Electromagnetic Parameters as a function of Frequency, Soil Density and Soil Moisture". Proc. IEEE. 62. pp.98-103, 1974.

Hoekstra, P. and Delaney, A. (1974). "Dielectric properties of soils at UHF and microwave frequencies". J. Geophys. Res.79; 1699-1708.

Jackson, T.J. and Schmugge, T.J. (1989). "Passive Microwave remote sensing system for soil moisture : Some supporting research". IEEE Trans. Geosci. Remote Sensing, 27 : 225-235.

Jackson, T.J. (1990). "Laboratory evaluation of a field - Portable dielectric/Soil moisture probe". IEEE Trans. Geosci. Remote sensing, 28 : 241-245.

Jonsher, A.K. "Nature" 267, pp.673. 1977.

Karen, M., Germain, S.T. and Swift, C.T. (1993). "Determination of dielectric constant of young sea ice using microwave spectral radiometry". J. Geophysical Res., 98: 4675-4679.

Karolkar, B. & J. Behari, "Biological tissue characterization at microwave frequencies". IEEE Trans Micro Theo. Tech. Vol. MTT-33, pp.64-66, 1985.

Kendra, J.R.; Ulaby, F.T. and Sarabandi, K. (1994). "Snow probe for in situ determination of wetness and density". IEEE Trans. Geosci. Remote Sensing 32: 1152-1159.

Leschanskii Yu.I., G.N. Lebedeva and F.D. Schumilin. "Electric Parameters of sandy and loamy soils in the range of Centimeter, Decimeter and Meter wavelengths". Izvex. Vuz. Uchef. Zoved. Rdiophy., 14. pp.562-569, 1971.

Low, P.F. "Physical Chemistry of clay water interactions". Advan. Agron. 13, pp.269-327. 1961.

Lytle, V.I. and Jezek, K.C. (1994). "Dielectric permitivity and scattering measurements of Greenland firn at 26.5 - 40 GHz. IEEE Trans Geosci. Remote Sensing 32: 290-295.

Matzler, C. (1994). "Microwave (1-100 GHZ) dielectric model of leaves". IEEE Trans. Geosci. Remote Sensing; 32 : 947-949.

Matzler, C. (1996). "Microwave Permitivity of dry snow". IEEE Trans. Geosci. Remote Sensing, 34 : 573-581.

Morris, R.C. and Fraley, L. (1994). "Soil permeability as a function of vegetation type and soil water content". Health Physics. 66 : 691-698.

Motla, J., Ibarra, A., Margineda, J. and Hernandez, A.(1993). "Dielectric property measurement system at cryogenic temperatures and microwave frequencies". IEEE. Trans. Instru. Measurement 42: 817-821.

Newton, R.W., Black, Q.R., Makanvand, S., Blanchard, A.J. and Jean, B.R. (1982). "Soil moisture information and Thermal microwave emission". IEEE Trans. Geosci. Remote Sensing, GE-20:275-281.

Ngai R.M., A.K. Jonsher, C.T. White. <u>Nature</u> 277. pp.185. 1979.

Njoku, E.G. and O'neill, P.E. (1982). "Multifrequency microwave radiometer measurements of soil moisture". <u>IEEE Trans, Geosci. Remote Sensing</u>, GE-20, 468-474.

Rao, P.V.N., Raju, C.S. and Rao, K.S.(1990). "Microwave Remote Sensing of soil moisture : Elimination of texture effect". <u>IEEE Trans. Geosci. Remote Sensing</u>, 28:148-151.

Roberts, S. & A.R. Von Hippel. "A new method for measuring dielectric constant and loss tangent in the range of EM waves". <u>J. Appl. Phys</u>. Vol.17, pp.610-645. 1946.

Rao, K.S., Raju, S. and Wang, J.R. (1993). "Estimation of soil moisture and surface roughness parameters from backscattering co-efficient". <u>IEEE Trans. Geosci. Remote Sensing</u>, 31 : 1094-1099.

Rouse, J.W. (1983). Comments on "The effects of texture on microwave emission from soils". <u>IEEE Trans. Geosci. Remote Sensing</u>, GE-21 : 508-511.

Saatchi, S.S., Le Vine, D.M. and Long, R.H. (1994). "Microwave backscattering and emission model for grass canopies". <u>IEEE Trans. Geosci. Remote Sensing</u>, 32 : 177-186.

Schmugge, T.J. (1983). "Remote sensing of soil moisture : Recent advances". <u>IEEE Trans. Geosci. Remote Sensing</u>, GE-21 : 336-344.

Schmugge, T.J. and Jackson T.J. (1992). "A dielectric model of the vegetation effects on the microwave emission from soils". <u>IEEE Trans. Geosci. Remote Sensing</u>, 30: 757 - 760.

Scott, W.R. and Smith, G.S. (1992). "Measured electrical constitutive parameters of soil functions of frequency and moisture content". <u>IEEE Trans. Geosci. Remote Sensing</u>, 30 : 621-623.

Shutko, A.M. and Reutov, E.M. (1982). "Mixture formulas applied in estimation of dielectric and radiative characteristics of soils and grounds at microwave frequencies". IEEE Trans. Geosci. Remote Sensing, GE-20: 29-32.

Straub, A. (1994). "Boundary element modelling of a capacitive probe for in situ soil moisture characterization". IEEE Trans. Geosci. Remote Sensing, 32: 261-266.

Stuchly, M.A. et al. "Coaxial line reflection methods for measuring dielectric properties of biological tissues at radio and microwave frequencies: A Review". IEEE Trans. Instr. and meas vol. IM-29. No.3, pp.176-183. 1980.

Stuchly, S.S., Stuchly, M.A. and Carraro, B. "Permittivity measurements in a resonator terminated by an infinite sample". IEEE Instr. Meas. Vol. IM-27, pp.436-439, 1978.

Stuchly, S.S. et al. "A method for measurement of the permittivity of thin samples". J. Microwave Power. Vol.14, pp.7-13. 1979.

Suber, W.H. & G.E. Crouch. "Dielectric measurement methods for solids at Microwave frequencies". J. Appl.Phys. Vol.19, pp.1130-1135. 1948.

Ulaby, F.T., Razani, M. and Dobson, M.C. (1983). "Effect of vegetation cover on the microwave radiometric sensitivity to soil moisture". IEEE. Trans. Geosci. Remote Sensing, GE-21:51-61.

Van Loon R. & J. Finsey. "The Precise microwave permittivity measurements of liquids using a multipoint technique and curve fitting procedures". J. Phy. D. Vol.8 pp.1232-1243. 1975.

Wang, J.R., T. Schmugge and D. Williams, "Dielectric constants of soils at microwave frequencies - II". NASA Tech, paper 1238, Godlard Space Flight Center. Greenbelt, MD. 1978.

Wang, J.R. and T.J. Schmugge. "An Empirical Model for the complex Dielectric Permittivity of soïls as a function of water content". *IEEE Trans. Geosci. Remote Sensing*. GE-18, pp.288-295, 1980.

Wang, J.R. "The Dielectric Properties of Soil-water mixtures at microwave frequencies". *Radio Sci*. 15 M. 977-985. 1980.

Wang, J.R., O'neill, P.E., Jackson, T.J. and Engman, E.T. (1983). "Multifrequency measurements of the effects on soil moisture, soil texture and surface roughness". *IEEE Trans. Geosci. Remote Sensing*, GE-21 : 44-50.

Wang, J.R. (1987). "Microwave emission from smooth bare fields and soil moisture sampling depth". *IEEE Trans. Geosci. Remote Sensing*, GE-25 : 616-621.

Wegmuller, U. Mitzler, C., Huppi, R. and Schanda, E. (1994). "Active and passive microwave signature catalog on bare soil (2-12 GHz)". *IEEE Trans. Geosci. Remote Sensing*, 32: 698-702.

Procedure for Texture Analysis of the Samples

The texture analysis of the samples were carried out by the Buoyoucos hydrometer method (cf: Allen, 1974).

<u>Reagents used</u>

Calgon, 5% w/v

50 g of Calgon was dissolved in distilled water.

Na_2CO_3 was added to bring the final pH to 9. Then the solution was diluted to 1 litre.

(Calgon is mainly Sodium hexametaphosphate and was used as the dispersing agent.)

<u>Procedure</u>

50 g of air-dried 2 mm sieved soil samples were weighed into the container of a high speed stirrer.

25 ml 5% Calgon and 400 ml tap water were added.

The soil sample was dispersed thoroughly by stirring for 15 min and transferred to a 1 litre cylinder and diluted to mark. The mixture was stirred by a paddle for 1 minute and the timing for Buoyoucos soil hydrometer readings commenced.

The readings were taken as follows (introducing the hydrometer 20 sec before reading):

B   : 4 min 48 sec   Silt and Clay

A   : 5 hours   Clay

The temperature of the suspension was noted after each reading and 0.3 units added or substracted for every degree above (or below) 19.5°C.

Calculations

If 50 g soil are dispersed in 1 litre and,

B   = hydrometer reading (gl^{-1}) after 4 min 48 sec.

A   = hydrometer reading (gl^{-1}) after 5 hours then.

$$Clay\ (\%) = \frac{A\ (gl^{-1}) \times 100}{50} - 1$$

(where 1 = Calgon correction)

$$Silt + Clay\ (\%) = \frac{B\ (gl^{-1}) \times 100}{50} - 1$$

Silt (%)   = (Silt + Clay) (%) - Clay (%)

and, Sand (%)   = 100 - (Silt + Clay) (%)

N.B: Froth produced during the mixing process through mechanical stirring was dispensed by adding a few drops of amyl alcohol before inserting the hydrometer.

Program (in pascal) to calculate the value of dielectric permittivity·by the two-point method:

```pascal
begin
write('Q%');
end.
tput);

var lambda_c,lambda_g,k          : real;
    gamma,vswr,d,dr,l,phi,x      : array [1..5] of real;
    A,B,C,inv_C,Psi              : array [1..5] of real;
    no,s,j                       : integer;
    y,av_y,theta,av_theta        : real;
    epsilon1,epsilon2            : real;
    x_pair, theta_pair           : array[1..5,1..2] of real;

begin
    writeln('Enter the no. of samples : ');
    readln(no);
    writeln('Enter lambda_c : ');
    readln(lambda_c);
    writeln('Enter lambda_g : ');
    readln(lambda_g);
    k := (2 * 3.14) /  (lambda_g);
    writeln;

    for j := 1 to no do
    begin
        writeln('Enter values of VSWR,D,Dr,l for sample no.
',j,' : ');
        readln(vswr[j],d[j],dr[j],l[j]);
        writeln
    end;

    for j := 1 to no do
    begin
        gamma[j] := (vswr[j] - 1) / (vswr[j] + 1);
        phi[j] := 2 * k * (d[j] - dr[j] -l[j]);
```

```
        x[j]    := 1 + gamma[j] * gamma[j] + 2 *  gamma[j]  *
        cos(phi[j]);
        A[j]    := -(lambda_g * gamma[j]  *  sin(phi[j]))  /
        (3.14 * l[j] * x[j]);
        B[j]    := -(lambda_g * (1 - gamma[j] * gamma[j]))  /
        (6.28 * l[j] * x[j]);
        C[j] := sqrt(A[j] * A[j] + B[j] * B[j]);
        Psi[j] := arctan(B[j] / A[j]) * (180 / 3.14);
        inv_C[j] := 1 / C[j]
    end;


    writeln;
    writeln('         C          Psi         1 / C       ');
    for j := 1 to no do
    begin
writeln(' ',C[j]:6:4,'   ',Psi[j]:6:4,'     ',inv_C[j]:6:4);
        writeln
    end;


    for j := 1 to no do
    begin
        writeln('Enter the two values of x for sample no.
',j,' : ');
        readln(x_pair[j,1],x_pair[j,2]);
        writeln('Enter the two values of theta for sample
no. ',j,' : ');
        readln(theta_pair[j,1],theta_pair[j,2])
    end;


    writeln;
    writeln('         Y            THETA_PRIME          ');
    writeln;
    for j := 1 to no do
    begin
        for s := 1 to 2 do
        begin
            y := (x_pair[j,s]) / (k * l[j]);
            y := y * y;
            theta := 2 * (theta_pair[j,s] - 90);
            writeln('      ',y:6:4,'          ',theta:6:4);
        end;
        writeln;
    end;

    writeln('Enter the average value of y : ');
    readln(av_y);
    writeln('Enter the average value of theta : ');
    readln(av_theta);
```

```pascal
    av_theta := (3.14 * av_theta) / 180;

    y := lambda_g / lambda_c;
    y := y * y;
    epsilon1 := (av_y * cos(av_theta) + y) / (1 + y);
    epsilon2 := -(av_y * sin(av_theta)) / (1 + y);
    writeln;
    writeln('Epsilon1 :  ',epsilon1:6:4,'   Epsilon2  :
',epsilon2:6:4);
    readln;

end.
```

** **Program to calculate the value of dielectric constant by the Single-horn Reflectometry method (in fortran 77)**

```fortran
      complex Roh,r1,r2
      real ds,dm, vs, vm, lambda, height
      real phi, delx, R, dphi
      real ccc, sss

      write(*,*) 'Type the values of ds dm vs vm lambda and height'
      read(*,*) ds,dm,vs,vm,lambda

      delx = abs(ds - dm)
      write(*,*) 'value of delta x is='
      write(*,*) delx

      dphi = (4.0*(22.0/7.0) * delx)/lambda
      phi = 22.0*dphi/(180.0*7.0)

      write(*,*) ' The value of phi is ='
      write(*,*) dphi

      R = ((vs-1.0)*(vm+1.0))/((vs+1.0)*(vm-1.0))
      write(*,*) 'The value of Roh is = '
      write(*,*) R
      ccc= abs(cos(phi))
      sss= abs(sin(phi))

      r1 = 1.0 +R*cmplx(ccc, sss)
      r2 = 1.0 -R*cmplx(ccc, sss)

      Roh = (r1/r2)*(r1/r2)

      write(*,*) 'The value of Dielectric constant is '
      write(*,*) Roh


      stop
      end
```